

## Article

# Testing the mHM-MPR Reliability for Parameter Transferability across Locations in North–Central Nigeria

Kingsley Nnaemeka Ogbu <sup>1,2,3,\*</sup>, Oldrich Rakovec <sup>2,4</sup> , Pallav Kumar Shrestha <sup>2</sup>, Luis Samaniego <sup>2</sup> , Bernhard Tischbein <sup>1</sup>  and Hadush Meresa <sup>1</sup>

<sup>1</sup> Center for Development Research—ZEF, University of Bonn, 53113 Bonn, Germany

<sup>2</sup> Helmholtz Centre for Environmental Research—UFZ, 04318 Leipzig, Germany

<sup>3</sup> Faculty of Engineering, Nnamdi Azikiwe University, PMB 5025, Awka 420001, Nigeria

<sup>4</sup> Faculty of Environmental Sciences, Czech University of Life Sciences Prague, 16500 Prague-Suchdol, Czech Republic

\* Correspondence: s7kiogbu@uni-bonn.de

**Abstract:** Hydrologic modeling in Nigeria is plagued by non-existent or paucity of hydro-metrological/morphological records, which has detrimental impacts on sustainable water resource management and agricultural production. Nowadays, freely accessible remotely sensed products are used as inputs in hydrologic modeling, especially in regions with deficient observed records. Therefore, it is appropriate to utilize the fine-resolution spatial coverage offered by these products in a parameter regionalization method that supports sub-grid variability. This study assessed the transferability of optimized model parameters from a gauged to an ungauged basin using the mesoscale Hydrologic Model (mHM)—Multiscale Parameter Regionalization (MPR) technique. The ability of the fifth generation European Centre for Medium-Range Weather Forecasts Reanalysis product (ERA5), Climate Hazards Group InfraRed Precipitation with Station data (CHIRPS), Global Precipitation Climatology Centre (GPCC), and Multi-Source Weighted-Ensemble Precipitation (MSWEP) gridded rainfall products to simulate observed discharge in three basins was first assessed. Thereafter, the CHIRPS rainfall product was used in three multi-basin mHM setups. Optimized model parameters were then transferred to independent basins, and the reproduction of observed discharges was assessed. Kling–Gupta Efficiency (KGE) scores showed improvements when mHM runs were performed using optimized parameters in comparison to using default parameters for discharge simulations. Optimized mHM runs performed reasonably (KGE > 0.4) for all basins and rainfall products. However, only one basin showed a satisfactory KGE value (KGE = 0.54) when optimized parameters were transferred to an ungauged basin. This study underscores the utility of the mHM-MPR tool for parameter transferability during discharge simulation in data-scarce regions.

**Keywords:** CHIRPS; streamflow; mHM; MPR



**Citation:** Ogbu, K.N.; Rakovec, O.; Shrestha, P.K.; Samaniego, L.; Tischbein, B.; Meresa, H. Testing the mHM-MPR Reliability for Parameter Transferability across Locations in North–Central Nigeria. *Hydrology* **2022**, *9*, 158. <https://doi.org/10.3390/hydrology9090158>

Academic Editor: Monzur A. Imteaz

Received: 25 July 2022

Accepted: 23 August 2022

Published: 2 September 2022

**Publisher's Note:** MDPI stays neutral with regard to jurisdictional claims in published maps and institutional affiliations.



**Copyright:** © 2022 by the authors. Licensee MDPI, Basel, Switzerland. This article is an open access article distributed under the terms and conditions of the Creative Commons Attribution (CC BY) license (<https://creativecommons.org/licenses/by/4.0/>).

## 1. Introduction

The declining economic conditions in many sub-Saharan African (SSA) countries have resulted in about 50–60% of their workforce depending on agriculture (subsistence farming) as a source of livelihood [1]. A nation's agricultural sector is important for ensuring food security, mental health, the health of its population, economic stability, and national development. In Sub-Saharan Africa (SSA), the agriculture production per capita trend has declined since 1960, resulting in 30% of its population being food insecure [2]. Farming is largely characterized by rain-fed agriculture and is practised majorly at the subsistence level. Sub-Saharan African countries import wheat, fertilizer, and vegetable oil from Ukraine and Russia. Unfortunately, the ongoing Ukraine–Russian war has disrupted food importation, thereby increasing already high food prices and worsening food security for millions of the population. In the era of increasing global warming, rainfall variability,

and more frequent hydrologic extremes (flood and drought), the source of livelihood of a great majority of the population in this region is threatened [3]. These authors noted, in a study that analyzed rainfall observations over West Africa that the average annual rainfall during 1970–2009 was below the annual average recorded for the period 1900–1970. Other studies [4–6] projected significant and extensive impacts of climate change on agriculture due to reductions in the length of farming seasons, shifts in seasonality, more severe dry spells, heat stress, and an increase in water-stress risks.

The availability of high-quality rainfall data is essential for water-related research and to support policy-making [3,7–10]. An analysis of annual rainfall data in Nigeria for a period of 72 years (1916–1987) showed a decreasing trend over southern, middle belt, and northern Nigeria [11]. Many studies [12–16] reported significant variability in rainfall trends in different regions in Nigeria. In recent decades, economic instability, weak institutions, and inadequate infrastructure have led to a decline in rainfall-monitoring networks across Nigeria, posing great insecurity to water resource planning and management [1]. Additionally, the growing Nigerian population, expansion of urban areas, insufficient water governance, and lack of effective water laws have hindered the effective implementation of integrated water resources management (IWRM), resulting in more water-related issues [17,18]. Furthermore, the unavailability of observational hydro-met data has impeded hydrologic-related research efforts and consequently is increasingly exposing the population to risks of extreme hydrologic events, hunger, and economic instability [19].

The emergence of gridded rainfall products at high spatio-temporal resolutions and the development of distributed hydrological modeling procedures have created possibilities for water resource modeling in ungauged basins [9,20,21]. Spatial rainfall data provide homogenous spatial coverage over inaccessible locations and has an advantage over in situ gauged data. However, the application of remotely-sensed rainfall data for research and operational hydrology in Nigeria is scarce in published works of literature to date. Many studies [20,22–28] have shown that gridded rainfall datasets can satisfactorily replicate observed spatio-temporal characteristics of gauged in situ records although with reported inconsistencies. Detailed reviews of the characteristics and performance of gridded rainfall data are found in the literature [29–31]. However, notwithstanding the advances in the development of gridded rainfall products, they are rarely applied in operational hydrology due to inherent biases [20,32], hence the need for validation to identify which product suits a specific region or locality.

Realistic hydrologic simulations and forecasting are constrained largely by hydrologic model complexity and input-data requirements [33]. The paucity of hydro-meteorological records in data-scarce regions has hindered hydrologic modelling applications. However, many studies [34–37] have shown success in utilizing global meteorological datasets for water balance analysis in sub-Saharan Africa. These freely available datasets have proven to be suitable alternatives and have aided realistic hydrologic process simulation and a better understanding of hydrologic systems [38]. However, the utilization of remotely sensed data has increased model complexity and, consequently, the need for higher computational power [39], which is not always available in developing countries [40]. Furthermore, fully distributed hydrologic models exist to cope with available high-resolution inputs, but the issue of realistic process representation persists [41]. Many authors [39,41,42] noted that problems of model nonlinearity, scale, uniqueness, uncertainty, and equifinality had not been satisfactorily addressed by the development of these complex distributed hydrologic models and their application at the mesoscale. Issues of over-parameterization and equifinality of feasible solutions aid the production of unreliable hydrologic outputs even when a good fit between observed and simulated discharge is achieved, creating uncertainties [43]. Even when model parameters can be deduced through optimization these values cannot be transferred to ungauged basins or to other scales other than that used during model calibration [39,44,45]. It is against the background that the International Association of Hydrologic Sciences (IAHS) in 2012 initiated the Scientific decade of Prediction in Ungauged

Basins (PUB) in their efforts to encourage more hydrologic research aimed toward the understanding of hydrologic processes, especially in data-scarce basins [46].

Parameterization techniques that are geared toward reducing the number of free parameters and model complexity have been developed in the past [39,44,47]. For example, the soil and water assessment tool (SWAT) [48] model employs the hydrologic response unit (HRU) technique where a certain area of land use, soil, and slope are homogeneously grouped before model calibration. The hydrologic water balance is then modeled at the HRU level, as shown in many studies [36,49–54]. However, a major drawback of this approach is that those model parameters are not directly linked to physical basin properties [44]. Alternatively, distributed hydrologic models can also be parameterized using the multiscale parameter regionalization (MPR) method [39]. In this technique, a distributed hydrologic model can be calibrated by connecting the model parameters to the basin's physical characteristics by assuming a priori-defined relationship, e.g., pedotransfer function [55,56]. Several studies [39,44] reported that the strength of the MPR method lies in its ability to account for sub-grid variability of soil, land use, and elevation characteristics to support the transfer of model parameters to other scales or ungauged basins other than those used during model calibration.

The mesoscale Hydrologic Model (mHM) [39,44] employs the MPR technique to aid the transferability of parameters to other scales and ungauged basins. Detailed information on the MPR-mHM is explicitly explained by [39,44]. The mHM model has been successfully applied in approximately 220 basins in Germany [57], 300 pan-European union basins [58], the continental United States [59], as well as in South East Asia [60]. In contrast, there have only been a few applications of the mHM on the African continent at the time of writing this paper. In a study [1] in a few West African basins, mHM produced satisfactory results. Additionally, mHM was used to model hydrological processes in the Volta River Basin, Ghana [61,62]. Application of mHM in any basin within Nigeria has not been undertaken before or is not evident in scientific published literature. In light of this information and given the sparse network of hydro-meteorological facilities that exist in Nigeria at present, this study employs the mHM-MPR technique for hydrologic simulation under data-scarce conditions. This approach is apt taking into consideration the challenges to water resources development in Nigeria due to recent modifications in the climate system and its impact on rain-fed agriculture. Furthermore, the unavailability of in situ input datasets for realistic hydrologic modeling in Nigeria and the need for the application of distributed hydrologic models to take advantage of existing high-resolution spatial datasets will support reliable simulation of hydrologic extremes (flood and droughts). We believe that the ability of the MPR method to support sub-grid variability and effective representation of the landscape can address the challenge of estimating reliable hydrologic model parameters at the mesoscale in Nigeria. This study addresses the following research questions:

1. What is the performance of gridded rainfall datasets over Nigeria?
2. How does mHM perform across selected basins when forced with different gridded rainfall datasets?
3. What is the performance of mHM when parameters are transferred from gauged to ungauged basins?

## 2. Methods

### 2.1. Study Area

Nigeria is located between latitude 4° N–14° N and longitude 4° E–15° E (Figure 1). It is bordered in the north by the Sahara desert and in the south by the Atlantic ocean. Its geographical position gave rise to InterTropical Discontinuity (ITD), which controls the weather throughout the year. The ITD is the region of lowest atmospheric pressure which separates the dry northeast trade winds from the Sahara Desert from the wet southwest monsoon from the Atlantic Ocean [15]. Three major climatic zones subdivided latitudinally as presented by Omotosho and Abiodun [63] exist in Nigeria: Guinea coast (Latitude 4–8° N),

Savannah (8–11° N), and Sahel (11–14° N) (Figure 1). Distinct climate characteristics over these regions are described in an earlier study [9,64].

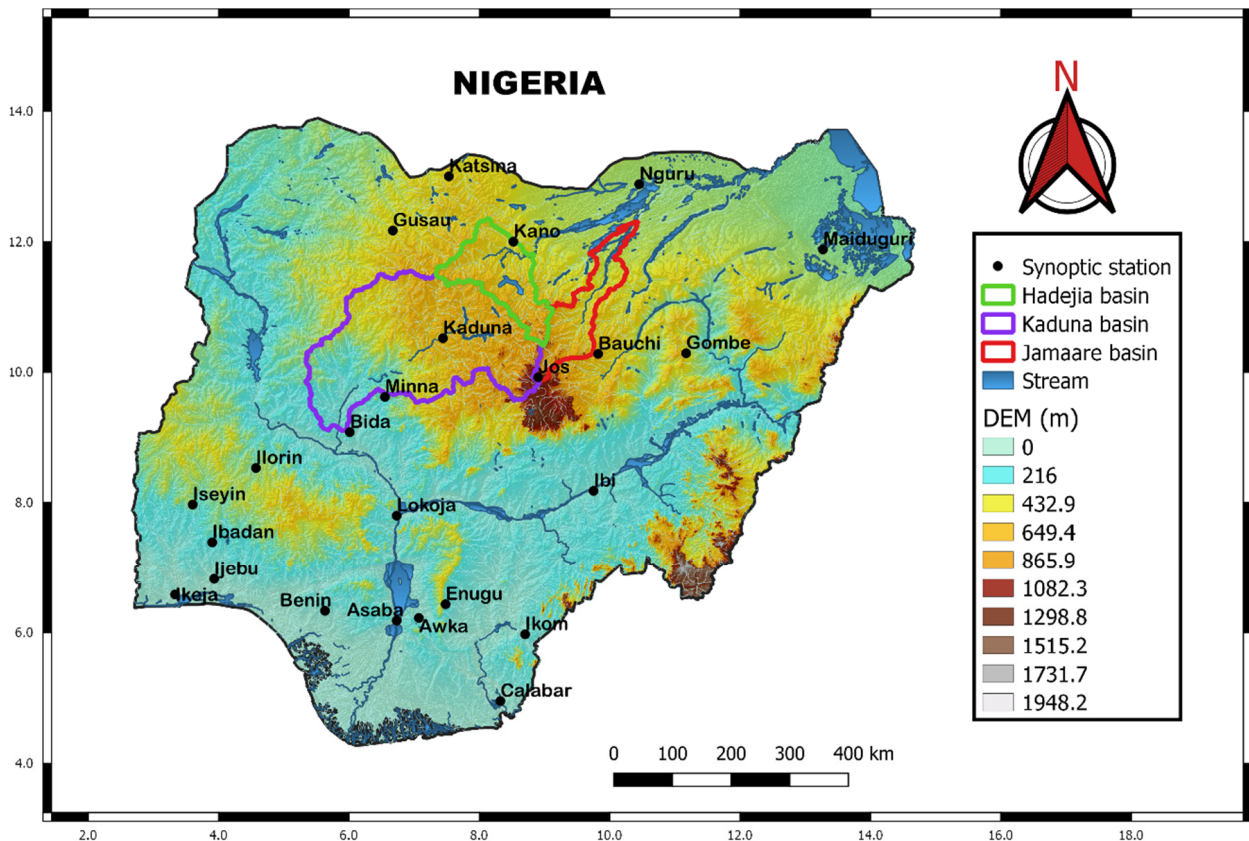


**Figure 1.** Map of Nigeria showing synoptic stations over three distinct climatic regions.

The study basins are the Kaduna (64,848 km<sup>2</sup>), Hadejia (16,820 km<sup>2</sup>), and Jamaare (13,929 km<sup>2</sup>) River Basin systems, which are located in the semi-arid north-central region of Nigeria (Figure 2). This region is characterized by sparse vegetation with scattered shrubs occasioned by frequent droughts and high rainfall variability [16,65]. The majority of the inhabitants dwelling in the Hadejia–Jamaare river basin are involved in cattle rearing, irrigated agriculture, cropland farming, and trading as sources of income [16]. During monsoon periods (April–September), farmers cultivate major crops, including sorghum, maize, millet, yams, soybean, and irrigated rice in the dry season (October–March). The Kaduna River is a critical water supply to the metropolis' inhabitants and for irrigated agriculture [13]. Both the Hadejia and Jamaare rivers discharge into Lake Chad but take their sources from both the Kano highlands and Jos Plateau, respectively [65]. Constructions of large-scale projects (e.g., dams) on these rivers (Shiroro dam on the Kaduna river; Tiga and Challawa Gorge dams on the Hadejia–Jamaare river system) [13,16,65] have impacted water flows and subsequently affected the micro-climate within the region. These dams were not represented during the modeling process due to the lack of a dam/reservoir component in mHM. The mean annual rainfall cycle over the North-central region of Nigeria is about 700–800 mm, with a unimodal peak in August. All study basins are located within the same agro-climatic region and are characterized by karstic geological formations and sparse vegetation as a result of long periods of dry season and short periods of monsoon season. The major differences between these basins are varied topography (Figure 2) and anthropogenic activities on the landscape. Large urban centres characterized by high human population and economic activities exist majorly within the Kaduna and Hadejia basins.

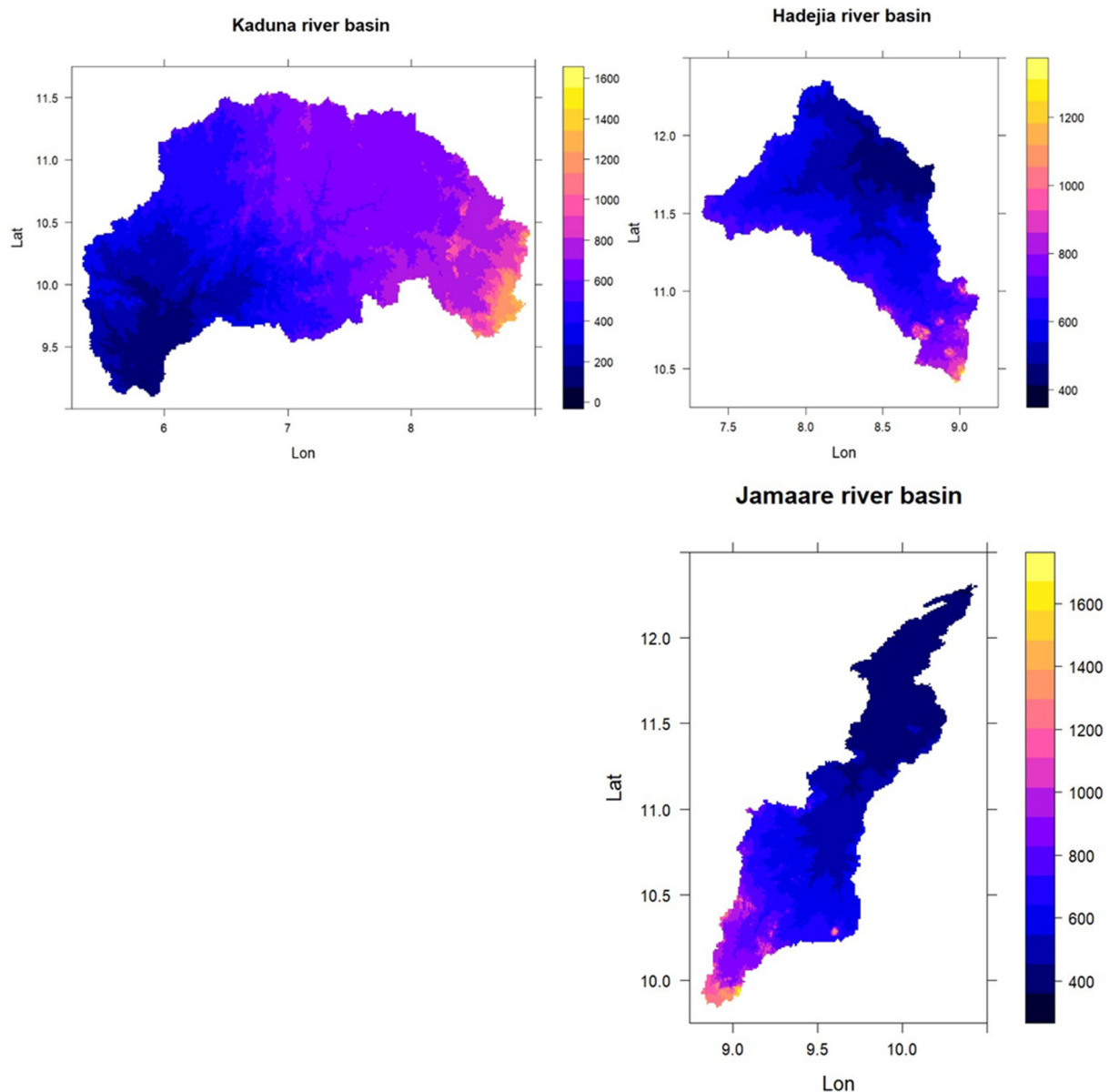


**Figure 2.** DEM for Kaduna (Basin No. 572), Hadejia (GRDC No. 1837410), and Jamaare river basins (GRDC No. 1837250) [66].

## 2.2. The mHM-MPR Structure: Description

The mesoscale Hydrologic Model (mHM) is a grid-based, spatially explicit conceptual hydrologic model forced with hourly or daily precipitation, temperature, and potential evapotranspiration datasets [39,44]. Its mathematical formulations are based on numerical approximations of dominant hydrologic processes as found in Hydrologiska Byråns Vattenbalansavdelning (HBV) [67] and Variable Infiltration Capacity (VIC) [68] models. The major components modeled in mHM include canopy interception, snow accumulation, soil moisture dynamics, infiltration, surface runoff, evapotranspiration, deep percolation, baseflow and flow routing, and groundwater storage [33]. In this study, potential evapotranspiration (PET) was estimated using temperature information obtained from ERA5 and read into mHM with aspect correction. A six-layer (50 mm, 150 mm, 300 mm, 500 mm, 1000 mm, and 2000 mm) infiltration capacity approach was used to calculate soil moisture in the root zone. Runoff routing from upper to lower grids through river networks was generated using the Muskingum–Cunge method. Interested readers can find a detailed mHM description in the previously published literature [39,44]. mHM code is open source

and is published in an online repository—[git.ufz.de/mHM](https://git.ufz.de/mHM). Version 5.11.0, accessed on 6 October 2020 was used for this research.

To describe the spatial dynamics of hydrologic processes per grid cell during hydrologic simulation, mHM requires 28 parameters (see Appendix A). Three mHM levels (Level-0, Level-1 and Level-2) are used to represent the spatial variability of state and input variables. Level-0 has the finest resolution and comprises morphological data such as elevation, land use, and slope, while Level-2 has the coarsest resolution and contains meteorological forcing data of precipitation, temperature, and evapotranspiration. Level-1 represents the dominant hydrologic processes and model outputs. Few mHM parameters (e.g.,  $\beta_2$ ,  $\beta_4$ ,  $\beta_9$ ,  $\beta_{11}$ ,  $\beta_{12}$ , and  $\beta_{14}$  (see Appendix A)) are assumed as global parameters because they do not exhibit spatial variability and, as such, are not regionalized [39].

Estimating each of the 28 mHM parameters for each grid modeling cell through calibration will result in over-parameterization [69]. To reduce the number of free calibrated parameters vis à vis the prediction uncertainty, MPR was employed to translate high-resolution input data variables into model parameters using transfer functions and upscaling operators [70]. This is performed in two steps, as reported in Kumar et al. [44]. In the first stage, mHM parameters evaluated at the input data scale (Level-0) are coupled with basin physical properties (e.g., terrain, soil texture, land cover, geology, etc.) through a priori established linear or non-linear transfer functions and a set of global parameters. In the final stage, these high-resolution parameters are upscaled to produce fields of effective parameters at the required hydrologic modeling spatial scale (Level-1) using upscaling operators such as arithmetic mean, geometric mean, or harmonic mean. Kumar et al. [69] summarized these two steps as follows:

$$\beta_{pi}(t) = O_p \langle \beta_{pj}(t) \forall j \in i \rangle_i$$

$$\beta_{pj}(t) = f_p(u_j(t), \gamma)$$

where  $p$  = number of model parameters;  $u_j$  =  $v$ -dimensional predictor vector for cell  $j$  at Level-0, which is contained by cell  $i$  at Level-1;  $O_p \langle \beta_{pj}(t) \forall j \in i \rangle_i$  = upscaling operator applied for regionalization of the parameter,  $p$ ;  $\gamma$  =  $s$ -dimensional vector of global parameters to be calibrated;  $v$  and  $s$  denote the total number of basin predictors and the total number of free parameters to be calibrated, respectively.

This procedure generates quasi-scale independent parameters which characterize sub-grid variability. In the end, approximately 64 global parameters (see Appendix B) were established over the whole modeling domain instead of estimating parameters at each grid cell independently. The advantage of this approach lies in the reduction of model complexity and over-parameterization, allowing transferability of model parameters across catchments, and improving model sub-grid variability and overall hydrologic simulation performance [39]. A calibration technique was then performed to adjust these parameters to simulate realistic historical hydrologic variables. Interested readers can find a detailed description of mHM-MPR in previous studies [39,44,59,71]. The mHM-MPR regionalization technique is superior to other regionalization schemes through the reduction of dimensionality of parameter space while maintaining sub-grid variability [70]. In a study [39] to assess the performances of the MPR and the Standard Regionalization (SR) methods using a distributed hydrologic model, MPR results showed superiority in many aspects. Furthermore, the MPR method was also tested with other hydrologic models over large continental domains with satisfactory results [71–73].

### 2.3. Data and Inputs

#### 2.3.1. Morphological Datasets

Digital elevation model (DEM) data at a resolution of  $0.002^\circ$  was obtained from the Global Multi-resolution Terrain Elevation Data (GMTED2010) [66]. The ArcMap geographical information system (GIS) was used to process slope, flow direction, aspect, and flow

accumulation for the study basins. Geological properties at 0.5° were obtained from the Global Lithological Map (Glim) version 1.0 database [74]

### 2.3.2. Soil Data

Soil information related to physical properties, including soil depth, bulk density, sand, and clay content, was obtained from SoilGrids database [75] at a resolution of 250 m for different soil layers and used during the model setup.

### 2.3.3. Landuse

In the mHM, land use data is aggregated and restricted to three (3) major classes: coniferous and mixed forest (class 1); impervious areas such as settlements, highways, and industrial parks (class 2); pervious areas representing fallow lands, agricultural lands, and pastures (class 3), using information obtained from the European Space Agency (ESA) at 300 m spatial resolution [76]. The monthly gridded leaf area index (LAI) was obtained from the Global Inventory Modeling and Mapping Studies (GIMMS) at 8 km spatial resolution [77].

### 2.3.4. Meteorological Data

Four (4) gridded precipitation products (ERA5 [31], CHIRPS [78], GPCC [79], and MSWEP [80]) (Table 1) comprising satellite, reanalysis, and gauge datasets were evaluated at the synoptic station scale (grid-to-point analysis) and over three distinct climatic regions in Nigeria. These products were selected based on their performance in previous studies [3,9,38] in the West African sub-region. These studies further noted that the GPCC, for example, satisfactorily captures the high variability that characterizes West African rainfall events. This robustness by the GPCC is not surprising as its development incorporates gauge records obtained from national meteorological agencies. Thermal infrared imagery and in situ station data are incorporated for the development of CHIRPS gridded observations. MSWEP was produced by merging in situ gauge, satellite, and reanalysis rainfall estimates, while ERA5 was developed from historical records using advanced modeling and data assimilation systems. Daily rainfall data (1983–2013) from 24 synoptic stations (see Figure 1) were obtained from the Nigeria Meteorological (NiMet) Agency and used as references to evaluate these gridded datasets at the climatic region scale. The selection of this period (1983–2013) is a consequence of missing data for many locations. Statistical metrics such as the Kling–Gupta efficiency (KGE) [81], Pearson correlation coefficient ( $r$ ), per cent bias (PBIAS), and root mean square error (RMSE) [82] were used to assess model performance against in situ gauge observations. The KGE addresses several limitations of the NSE and is based on the decomposition of NSE into three components (correlation, variability ( $\alpha$ ), and bias ( $\beta$ )). KGE values range from  $-\infty$  to 1, and KGE = 1 designate perfect agreement between predictions and observations. Beta ( $\beta$ ) is the ratio of the mean of the predicted values to the observed values and has an ideal value of 1 (i.e., ideal  $\beta = 1$ ), while alpha ( $\alpha$ ) is the ratio between the standard deviation of the predicted value and observed values. The ideal value for  $\alpha = 1$ . Pearson's correlation coefficient describes the degree of collinearity between model-simulated and observed time series records and ranges from  $-1$  to 1. No relationship exists between predicted and observed data when  $r = 0$ . On the other hand, a perfect positive or negative relationship exists when  $r = 1$  or  $-1$ , respectively. PBIAS quantify the likelihood of predicted values deviating from their observed counterparts. In this case, PBIAS = 0 indicates accurate model prediction, while negative and positive values signify model overestimation and underestimation biases, respectively. RMSE measures the standard deviations of the prediction errors. A smaller RMSE value designates better model performance.

$$KGE = 1 - \sqrt{(r - 1)^2 + (\alpha - 1)^2 + (\beta - 1)^2},$$

where  $r$  is the linear correlation between simulation and observation,  $\alpha$  is the flow variability, and  $\beta$  is the bias ratio.

$$r = \frac{\sum_1^n (O_i - \bar{O}) (S_i - \bar{S})}{\sqrt{\sum_1^n (O_i - \bar{O})^2 \sum_1^n (S_i - \bar{S})^2}},$$

$$PBIAS = \frac{\sum_{i=1}^n O_i - S_i}{\sum_{i=1}^n O_i} \times 100,$$

$$RMSE = \sqrt{\frac{1}{n} \sum_{i=1}^n (O_i - S_i)^2},$$

where  $O$  and  $S$  are observed and simulated values, respectively, and  $i$  is time steps.

**Table 1.** Precipitation products evaluated in this study.

Precipitation Product	Data Sources	Spatial Coverage	Spatial Resolution
ERA5	Reanalysis	Global	0.25°
CHIRPS	Satellite, gauge, reanalysis	50° N–50° S	0.05°
GPCC	Gauge	90° N–90° S	1.0°
MSWEPv2.2	Satellite, gauge, reanalysis	Global	0.1°

### 2.3.5. Discharge Data

Daily discharge data for study basins obtained from the database of the World Meteorological Organisation German Global Runoff Data Center (GRDC) and Nigerian Hydrological Services Agency (NHISA) were used for mHM calibrations and validation (Table 2). GRDC documents river discharge data on behalf of the World Meteorological Organization and with the permission of national governments. The problem of missing data necessitated the use of different periods for each study basin during model calibration. The GRDC station No. 1837250 is hereafter named Basin 250, while GRDC Station No. 1837410 is hereafter named Basin 410 to correspond with the 3-digit Basin 572. We acknowledge the policy guiding the dissemination of GRDC data as documented on [https://www.bafg.de/GRDC/EN/01\\_GRDC/12\\_plcy/data\\_policy\\_node.html;jsessionid=D0D2E24F2991D2AE1C9FA4BEF25C995A.live11311/](https://www.bafg.de/GRDC/EN/01_GRDC/12_plcy/data_policy_node.html;jsessionid=D0D2E24F2991D2AE1C9FA4BEF25C995A.live11311/), accessed on 6 October 2020.

**Table 2.** Daily discharge data.

Basin Name	GRDC Station No	Period of Coverage	Station Name	Source
Jamaare	1837250 (250)	1983–1997	Kotagum	GRDC
Hadejia	1837410 (410)	1987–1991	Wudil	GRDC
Kaduna *	572	1989–1995	Wuya	NHISA, Nigeria

\* obtained from Nigeria Hydrological Services Agency (NHISA).

### 2.3.6. Hydrologic Modeling Framework

To guarantee some level of trust in the mHM results in this study, a modeling experiment was developed where the model output (discharge) was assessed for 12 different simulation runs while varying precipitation datasets (CHIRPS, ERA5, GPCC, and MSWEP) across 3 river basins and using default model parameters. Due to limited climate data availability, potential evapotranspiration was computed by applying the Hargreaves–Samani

method [83] driven with ERA5 daily mean temperature and daily temperature ranges for all model setups. Firstly, hydrologic simulations for each river basin were performed, forced separately with each gridded precipitation product while using default model parameter values. Secondly, all model setups were calibrated for discharge simulation using each gridded precipitation dataset. Performance in discharge simulations for different model setups (i.e., different precipitation datasets) was assessed using the Kling–Gupta efficiency [81] metric (Equation (1)). The choice of the KGE method stems from the fact that it addresses the limitations in NSE and is now the preferred choice for model calibration and evaluation [84]. Popular optimization algorithms which produce optimal solutions include shuffled complex evolution [85], adaptive simulation annealing [86], particle swarm optimization [87], covariance matrix adaptation evolution strategy [88], and dynamically dimensioned search [89] algorithms. Model optimization was performed using the Dynamically Dimensioned Search (DDS) algorithm. The DDS algorithm is more effective and well-suited for computationally intensive hydrologic modeling when compared to the shuffled complex evolution (SCE) optimization method. The DDS provides an automatic and faster stochastic neighborhood search method for finding the best parameter combinations within a user-set number of iterations during distributed hydrologic modeling [89]. Once the most performed gridded dataset is established, it is used in the next stage of modeling experimentation. Thirdly, a multi-basin mHM setup was developed by setting up the mHM for three different basin combinations (Basins 250 + 410, Basins 572 + 410, Basins 250 + 572) using only CHIRPS datasets to infer unique model parameter sets for every basin combination. Lastly, optimized parameter sets obtained from each of the two-basin combinations were used to simulate discharge in an independent third basin. This approach is necessary to assess the feasibility of transferring mHM optimized parameters to a different basin for stream discharge simulation.

### 3. Results and Discussion

#### 3.1. Gridded Precipitation Rainfall Products Performance

Daily gridded precipitation estimates (1983–2013) were obtained on a grid-to-point scale using the location of synoptic weather stations, as shown in Figure 1. Taylor diagrams depicting time series of daily gauge rainfall in comparison to grid-based products for stations within the Sahel, Savannah, and Guinea coast regions are presented in Figures 3–5, respectively.

Correlation and RMSE values for some selected synoptic stations within each of the three climatic zones, as presented in Figure 3 (Sahel), Figure 4 (Savannah) and Figure 5 (Guinea), show varying results without any particular order at daily temporal resolution. In the Sahel, only GPCC was able to record satisfactory correlation ( $r > 0.5$ ) and RMSE ( $RMSE > 12$ ) for all locations under consideration. This trend was also the same in the Savannah region with correlation values above 0.6 (i.e.,  $r > 0.6$ ) and lower RMSE values ( $RMSE > 9$ ). In the Guinea coast region, an acceptable result ( $r > 0.9$ ,  $RMSE > 5$ ) was only obtained in Lokoja (Figure 5).

Overall, GPCC showed consistent satisfactory performances in comparison to in situ station data, mostly in the Sahel (Figure 3) and Savannah (Figure 4) regions. Similar studies [90,91] exhibited the same performance when the GPCC dataset was evaluated against synoptic stations in Nigeria. These authors attributed the GPCC performances to the integration of in situ gauge rainfall records in its algorithm during development.

The general performances of the GPCC in many of the locations agree with the results of Ogunjo et al. [91] in their study to evaluate the performances of three gridded rainfall products over Nigeria. This performance is largely attributed to the incorporation of in situ rainfall observations within the GPCC computational algorithm. Other studies [38,92] showed similar trends concerning the GPCC's ability to reproduce station records.

The mean annual cycle of all precipitation datasets over each climatic zone was evaluated for both gauge and gridded rainfall data records. Results over the Sahel, Savannah,

and Guinea coast regions are presented in Figure 6, and the error indices are shown in Figure 7.

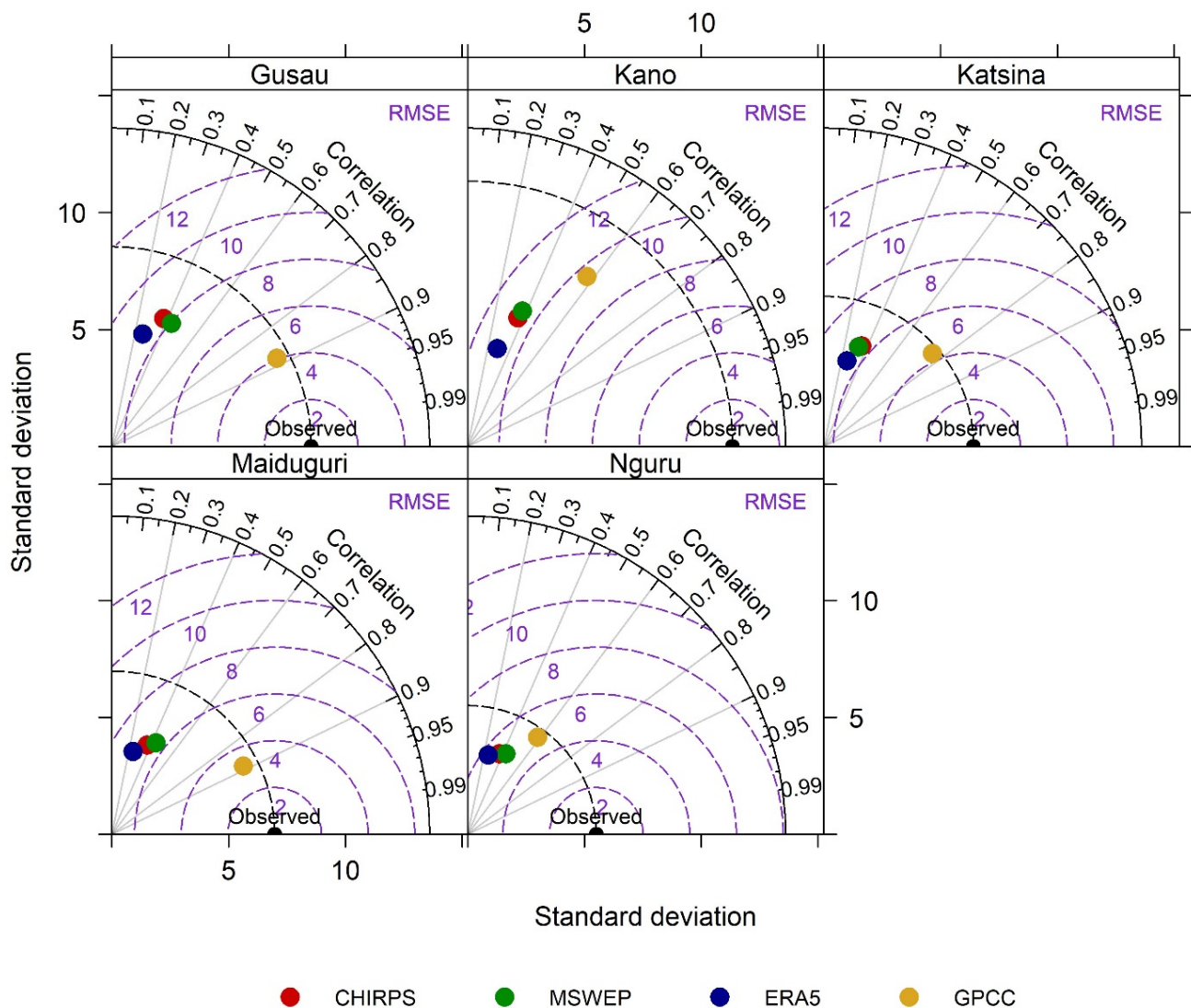


**Figure 3.** Taylor diagram of synoptic stations within the Sahel climatic zone.

The annual precipitation cycle of mean monthly rainfall for each of the three climatic regions implies that all grid-based products could reproduce observed rainfall trends and peaks, though with a varying magnitude of errors, as seen in Figure 7. This also signifies that these grid-based products captured the latitudinal oscillations of convective processes from southern latitudes to northern latitudes well, which characterize the west African monsoon. Furthermore, rainfall seasonality in all regions was well-reproduced by grid products under consideration in this study; the unimodal rainfall peak was reproduced in Sahel and Savannah regions, while bimodal peaks were shown by all grid-based products in the Guinea coast region. All gridded datasets recorded high KGE ( $KGE \geq 0.8$ ) and NSE values ( $NSE \geq 0.8$ ) in all climatic regions but were not presented in this study. Low RMSE ( $< 10$  mm) and bias ( $\pm 6\%$ ) values were recorded by the CHIRPS gridded data in all locations and showed its ability to reproduce the West African monsoon with low error margins. The acceptable performance of the CHIRPS dataset in this study is in agreement with other studies [20,93,94] carried out over the SSA region.

All precipitation products in the Savannah and Guinea coast regions (Figure 6) showed a nearly similar trend in comparison to in situ observations to those presented for the Sahel region. Satgé et al. [95] suggested that mismatches between satellite rainfall datasets and

observations, as is evident in the Sahel and Guinea coast regions (Figure 6), could be attributed to differences in reporting times for all datasets. In their study [94,95], satellite-based rainfall products (e.g., CHIRPS, MSWEP) showed overall better performance over reanalysis products which is in agreement with our findings in this study. In the Sahel, ERA5 gave RMSE > 25 and PBIAS > 20% (Figure 7) against lower values obtained for other products.

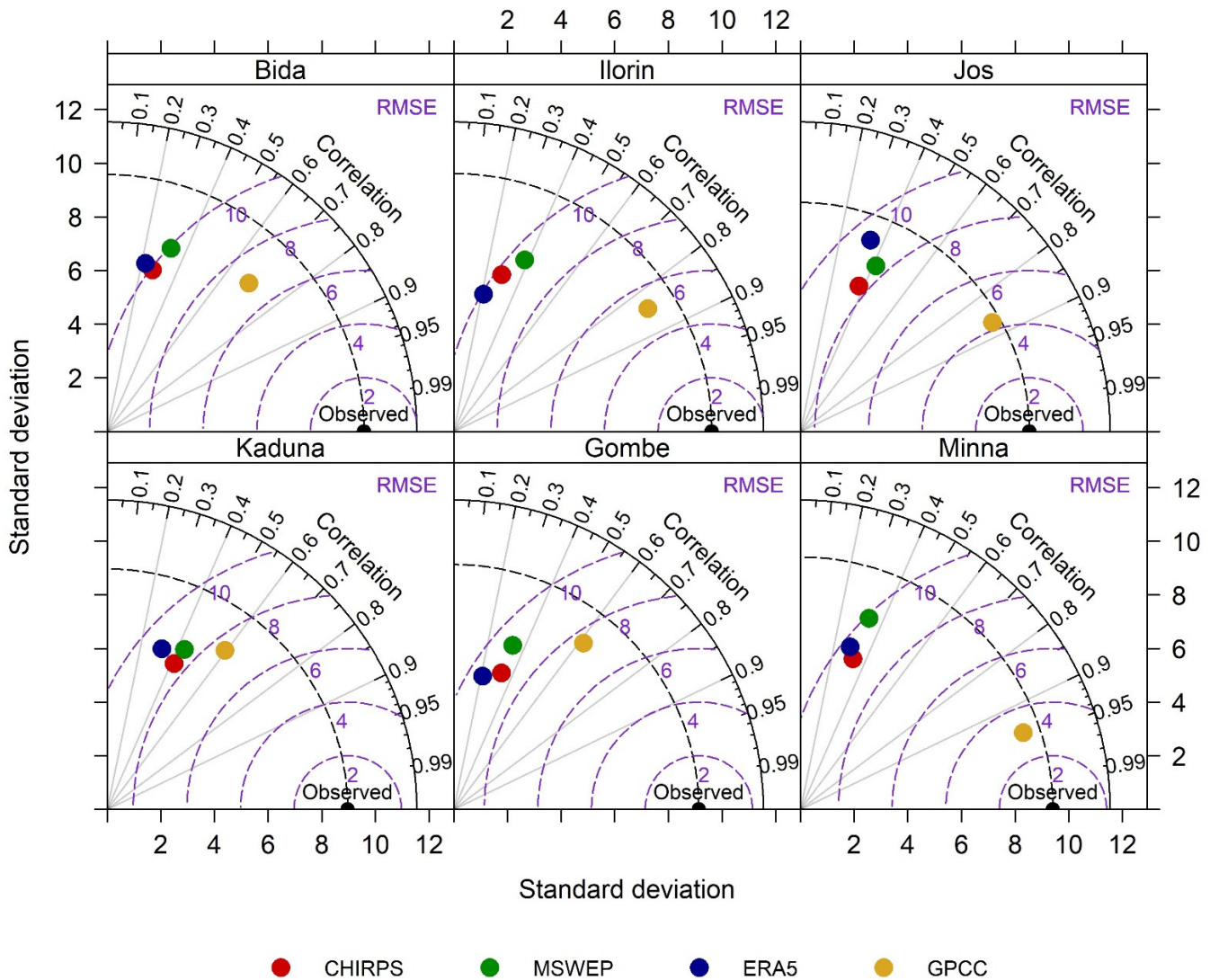


**Figure 4.** Taylor diagram of synoptic stations within Savannah climatic region.

### 3.2. Exploratory and Optimized Model Results

During mHM exploratory runs, discharge simulations were performed using default model parameters while varying precipitation inputs across the three different study basins. In all, 12 default model runs were carried out to evaluate simulated discharge results against observed discharge. The result of exploratory mHM simulations using default parameter values is shown in Table 3. To assess which gridded precipitation input reproduced gauged discharge time series, mHM was calibrated for each river basin while varying precipitation inputs. KGE values during optimized mHM runs are also shown in Table 3.

Discharge simulations in the Jamaare (Basin 250), Hadejia (Basin 410), and Kaduna (Basin 572) basins using default mHM parameters while varying precipitation inputs, as presented in Table 3, generally show poor KGE results. Acceptable KGE values, as recommended by Knoben et al. [84], were obtained for discharge simulation in the Jamaare river basin when forced with CHIRPS (KGE = 0.68437) and MSWEP (KGE = 0.65066). In Hadejia

and Kaduna river basins, none of the gridded rainfall products showed satisfactory results except ERA5 in the Hadejia basin ( $KGE = 0.68170$ ). Using  $KGE = 0$  as a threshold between good and bad model simulation in this study, negative  $KGE$  scores ( $KGE < 0$ ) obtained mostly in Hadejia and Kaduna basins designate poor model performance. Additionally, none of the poor-performing basins provided a  $KGE$  value greater than  $-0.41$ , and, as such, this signifies that the result did not improve upon using the mean as reported by Knoben et al. [84]. Overall, mHM exploratory (using default parameter values) results indicate unacceptable performance in almost all the basins modeled. These poor  $KGE$  results obtained while using default parameters are similar to those obtained in another mHM application [1] in West African Basins. The study of Poméon et al. [1] and our research share similarities; both applied mHM in West African Basins, and potential evapotranspiration data were read in with an aspect-driven correction. Both studies produced poor  $KGE$  values when mHM was driven with GPCP product in all basins using the default model setup. In this study, default mHM simulation results with regard to each meteo forcing are vague and unclear. Stream discharge dynamics were mostly captured in the Jamaare basin. Poor results obtained in the Hadejia and Kaduna basins could be attributed to the misrepresentation of dams/reservoirs existing in these locations.

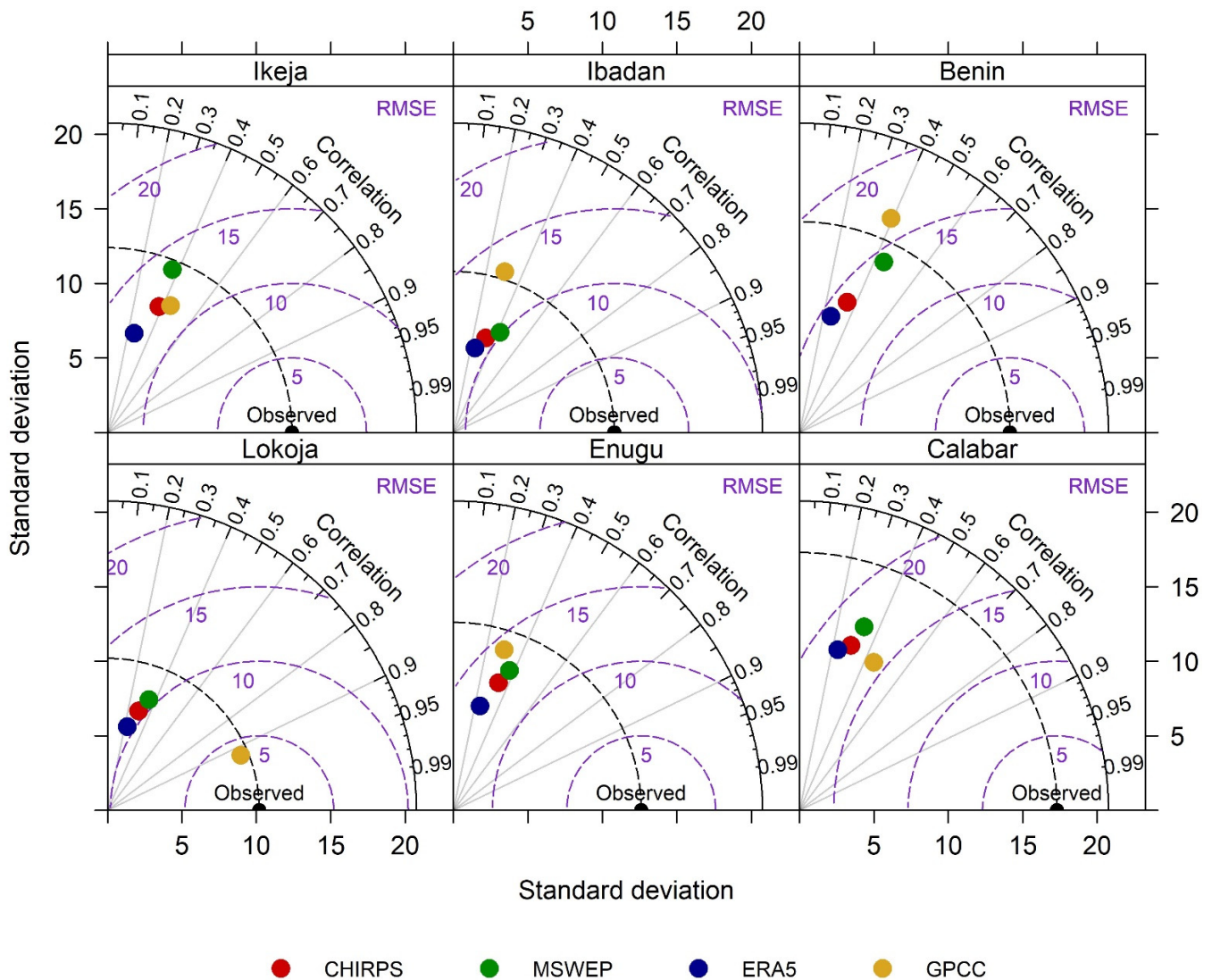


Figure 5. Taylor Diagram of Synoptic Stations within Guinea coast region.

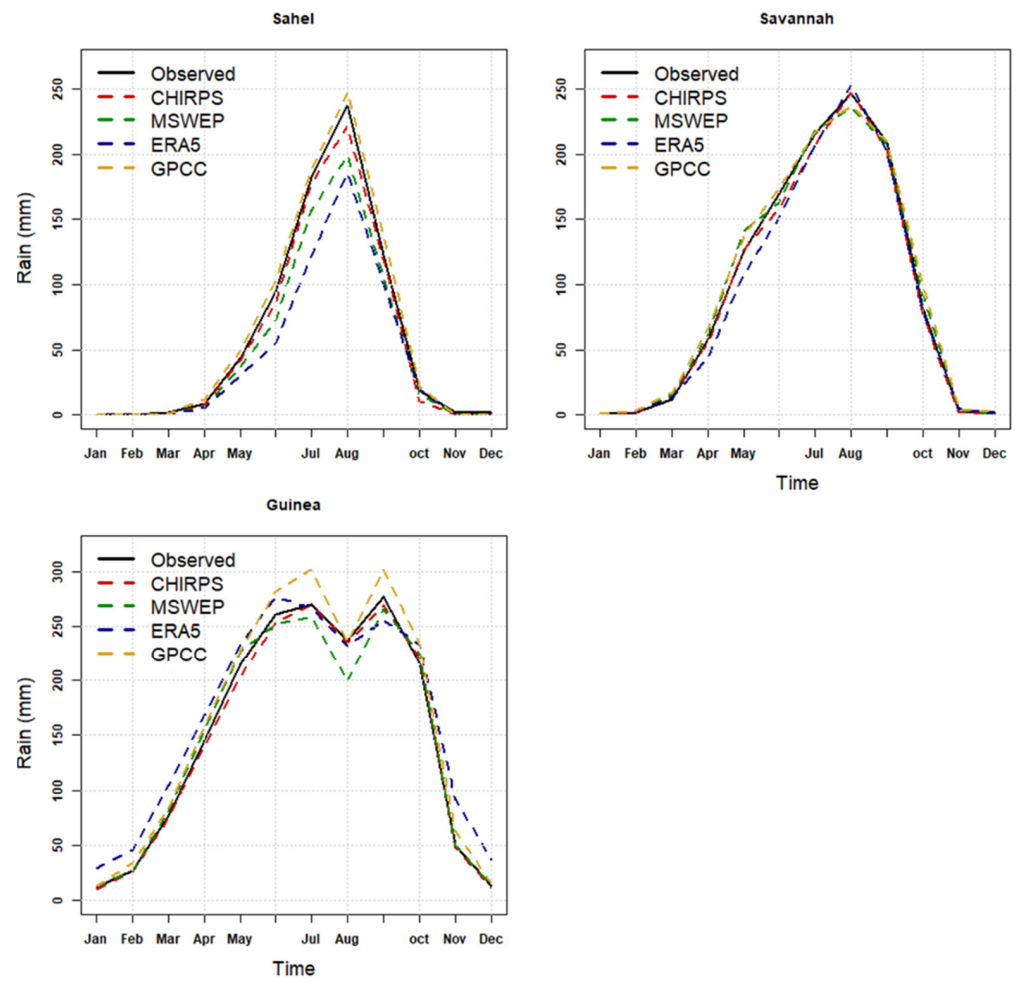


Figure 6. Mean annual cycle over the Sahel, Savannah, and Guinea coast region.

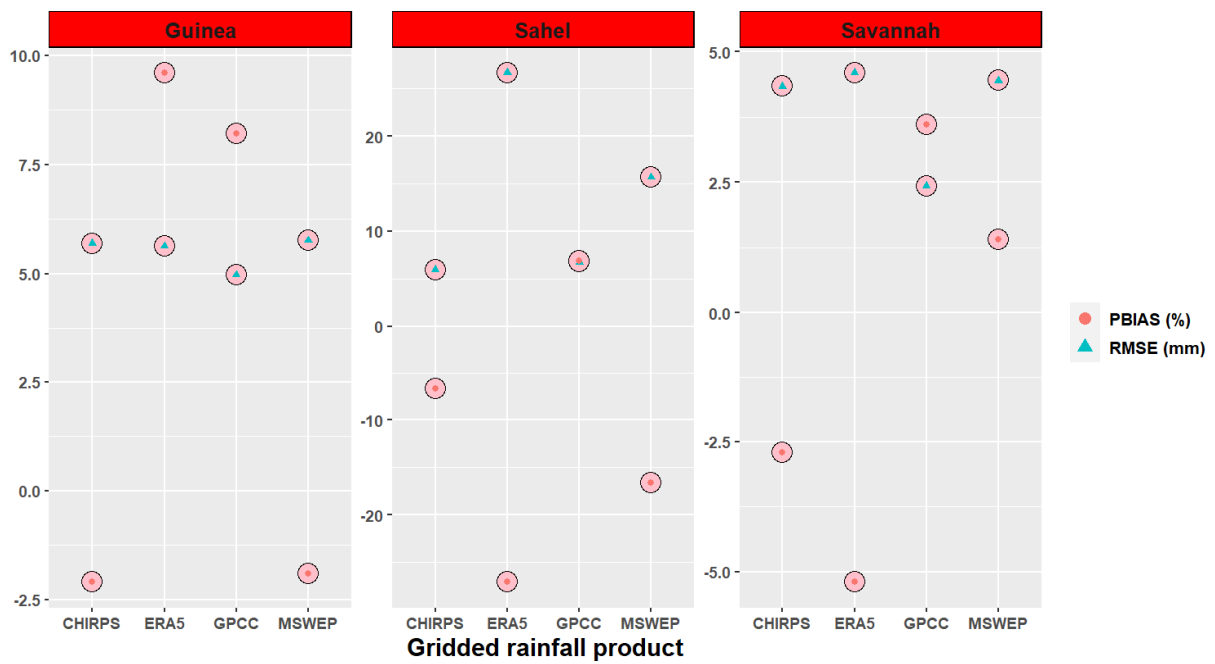


Figure 7. Error Indices for rainfall products.

**Table 3.** KGE results for default and optimized mHM discharge simulations.

Simulation Using Default mHM Parameters			Simulation Using Optimized mHM Parameters			Forcing
Jamaare (Basin 250)	Hadejia (Basin 410)	Kaduna (Basin 572)	Jamaare (Basin 250)	Hadejia (Basin 410)	Kaduna (Basin 572)	
0.68	−1.18	−2.22	0.79	0.66	0.51	CHIRPS
0.06	0.68	−1.78	0.75	0.64	0.44	ERA5
0.65	−0.53	−1.78	0.76	0.74	0.52	MSWEP
0.43	−1.34	−1.50	0.45	0.63	0.49	GPCC

On the other hand, optimized mHM discharge simulations showed significant improvements when compared with results from the default mHM parameter simulations. Satisfactory calibrated discharge results were produced by CHIRPS (KGE > 0.5) in all three basins, with ERA5 in Jamaare (KGE = 0.75) and Hadejia (KGE = 0.64). MSWEP produced a KGE > 0.5 in the three basins, while GPCC provided a KGE value of = 0.63 in the Hadejia river basin. In comparison with default mHM parameter simulation, optimized discharge simulation results (KGE values) showed an increase of 15.85% in Jamaare, 155.62% for Hadejia, and 123.11% in Kaduna basin when forced with CHIRPS. For ERA5, a decrease of 6.43% was obtained in Hadejia, while an increase of 1155.44% and 124.98% were observed in Jamaare and Kaduna basins, respectively. These improvements in discharge results, when compared to that from default mHM runs, were also obtained when optimizations were performed with MSWEP (17.31–241.1%) and GPCC (4.57–132.64%) forcings in the three basins. In general, optimized KGE results for all meteorologic products indicate agreement between simulations and observations. It is clear from this study that the calibrated mHM model performed well for discharge simulations. This performance is consistent with the studies of Poméon et al. [1] and Dembélé et al. [20], which showed acceptable discharge simulations in West Africa basins using optimized model parameter values. In this study, there was no clear pattern concerning high-performing rainfall products across all basins under consideration. As presented in Table 3 (for optimized mHM parameters), CHIRPS exhibited the highest KGE in the Jamaare basin, while MSWEP was best at performing in the Hadejia and Kaduna basins. Therefore, no particular rainfall products performed best across all locations. This finding aligns with the studies of Beck et al. [96] and Dembélé et al. [20]. These authors recommend rainfall product performance evaluation to select the most suitable for a specific location.

Daily hydrographs of simulated discharge against observations at Jamaare (Basin 250), Hadejia (Basin 410), and Kaduna (Basin 572) forced with the CHIRPS dataset are shown in Figure 8, respectively. Model performances for the three basins revealed acceptable values, but simulated peak flows in Hadejia and Kaduna basins were not successfully captured. These variations could be attributed to the quality of gauged station observations and the high uncertainties inherent in gridded precipitation records.

Generally, daily hydrographs obtained using optimized parameters forced with the CHIRPS dataset for Jamaare (Basin 250), Hadejia (Basin 410), and Kaduna (Basin 572) show acceptable fits between observed and simulated discharge. High correlation values ( $r > 0.5$ ) were recorded across the three hydrographs with Basin 250 showing high KGE (KGE = 0.79) and correlation ( $r = 0.86$ ) scores. Peak and low simulated flow followed the observed trend recorded in the Jamaare Basin more satisfactorily than displayed in the Kaduna and Hadejia basins. The study by Poméon et al. [1] also showed poor trend and peak flow representations in some of the West African basins under their consideration. These authors further observed discrepancies in mHM flow simulations in basins located within the same region. In this study, our hydrographs (Figure 8) also showed that optimized mHM performs acceptably in the Jamaare basin and poorly in the Hadejia and Kaduna basins. We agree with Poméon et al. [1] that several factors could be responsible: (1) several dams/reservoirs which exist within Hadejia and Kaduna basins were not represented in mHM. The Shiroro dam, located in the Kaduna basin, has a total reservoir capacity of 7,000,000,000 m<sup>3</sup>. The Challawa Gorge and Tiga Dams in the Hadejia basin contain

reservoirs that have a total volume of 930,000,000 m<sup>3</sup> and 1,968,000,000 m<sup>3</sup>, respectively. In addition to these large dams located in these two basins, many other medium-small size dams are also existing in this region. Consequently, mHM lack a reservoir component and does not simulate reservoirs and water abstracted for irrigation or domestic water supply purposes. (2) Secondly, data gaps and insufficient discharge time series impact model performance. Generally, improvements in KGE values from uncalibrated to optimized mHM runs underscore the benefit of the MPR technique for discharge simulation in the study region.

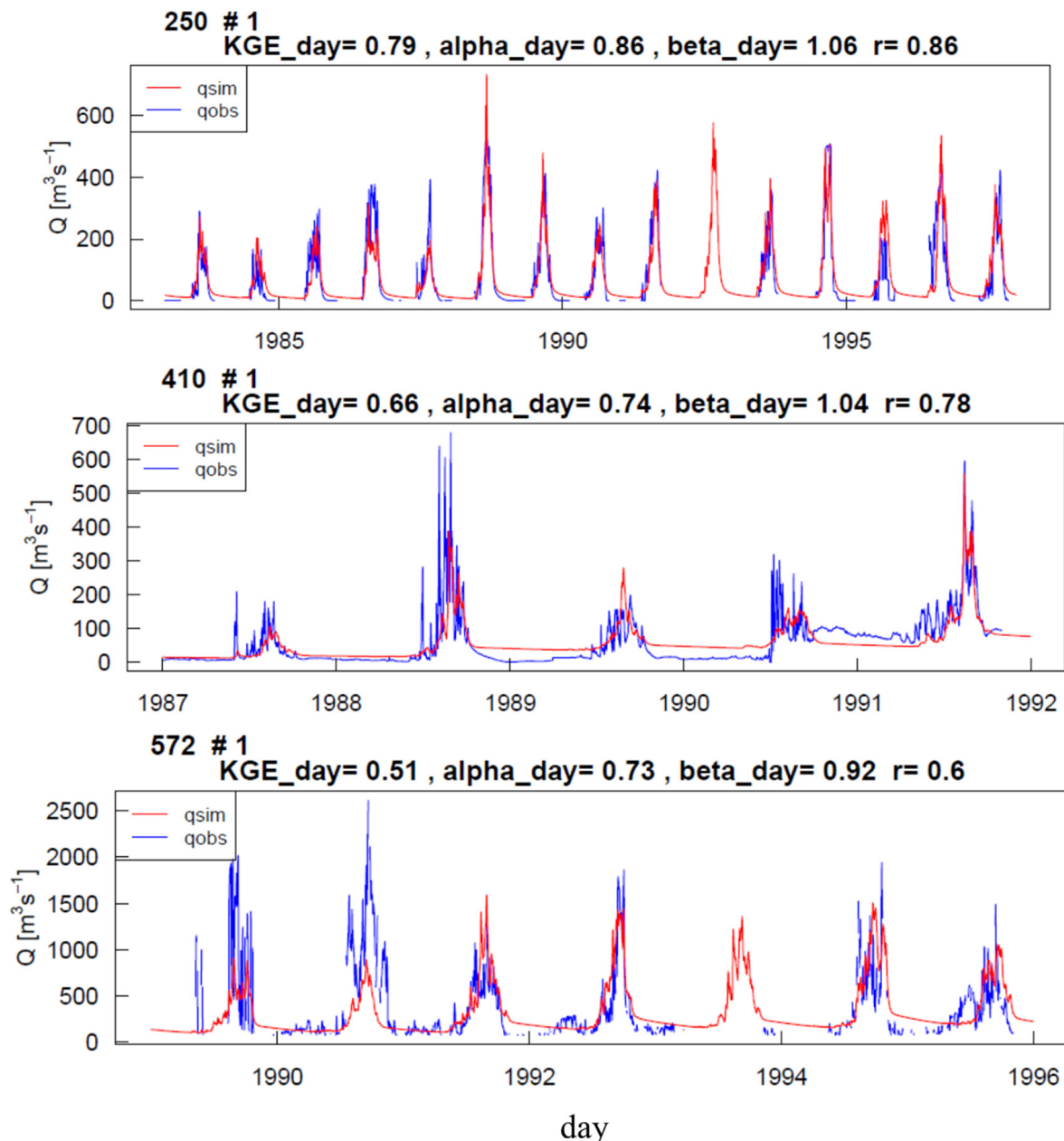


**Figure 8.** Hydrographs for Jamaare, Hadejia, and Kaduna basins forced with CHIRPS dataset.

### 3.3. Multi-Basin Optimization

A multi-basin mHM, comprising two basins (Basin 1 and Basin 2) each, was set up. A total of three different multi-basin combinations (Basins 250 + 410, Basins 572 + 410, and Basins 250 + 572) were created and forced with the CHIRPS precipitation product. Each of these model setups was calibrated using KGE as the objective function. Optimized model parameters were transferred to a different basin which was not considered during

model parameterization. Model evaluation was performed by assessing mHM capability in reproducing observed discharge in an independent basin using optimized model values from the multi-basin setup which is shown in Table 4. KGE values for each of the multi-basins (Basin 1 and Basin 2) combinations are presented in Table 4.

**Table 4.** Optimized mHM results (KGE) from multi-basin combinations.

Basin	Multi-Basin Combinations			Meteo
	Basin 250 + Basin 410	Basin 572 + Basin 410	Basin 250 + Basin 572	
1	0.33	0.51	−0.03	CHIRPS
2	0.64	0.51	0.58	

Having calibrated each of the multi-basin mHM setups for discharge simulation, optimized parameter values from Basin 250 + 410 were transferred to Basins 572 for discharge simulation. Additionally, calibrated mHM parameters from Basins 572 + 410 were used for flow simulation in Basin 250, while optimized parameters from Basin 250 + 572 were transferred to Basin 410. KGE results of these discharge simulations are provided in Table 5. Optimized model parameters from basin combination comprising of Basins 250 + 572 produced accepted KGE values.

**Table 5.** mHM validation results on independent basins.

Metric	Single Basin mHM Simulation			Meteo
	Basin 572	Basin 250	Basin 410	
KGE	0.02	−0.12	0.54	CHIRPS

Hydrographs of daily, monthly and annual flow cycle for Basin 410 (Hadejia River Basin) are shown in Figure 9. Hydrographs for Basin 572 and Basin 250 are not presented because they exhibited unsatisfactory KGE scores. Final values of optimized global parameters for all three basin setups are presented in Appendix B.

Optimized mHM parameters from different multi-basins were transferred to an independent basin to evaluate the predictive skill of mHM for discharge simulation in ungauged basins. KGE values obtained during optimization of multi-basin mHM runs forced with CHIRPS are shown in Table 3. Results from Table 4 for Basin 410 revealed an acceptable KGE (KGE = 0.54) when mHM was evaluated using optimized parameters which were obtained after calibration in Basin 250 + Basin 572. The monthly discharge (Figure 9) show slight underestimation of observed discharge but with acceptable performance (KGE = 0.61,  $r = 0.78$ ). The more desirable agreement exhibited at the monthly temporal resolution is a result of averaging the daily time series over the simulation period. This is comparable to a study by Zink et al. [57] At a daily time step, observed and simulated discharge exhibited a similar trend but with clear peak flow mismatches.

Overall, the feasibility of transferring mHM optimized parameters across different locations exhibited promising results only in the Hadejia basin. However, our study could not fully demonstrate the effectiveness of transferring optimized parameter sets to ungauged basins although these basins exist in the same agro-climatic region. This observation is also reported by Zelelew and Alfredsen [97]. These authors attributed this inconsistency to input data uncertainties, parameters interactions and model structure. In our case, integrating model parameter sets from two basins, which increased the parameter search space, failed to improve simulation results in Jamaare and Kaduna basins. The Acceptable KGE score obtained in the Hadejia basin by using an optimized parameter set from Kaduna and Jamaare could also be attributed to their domain size. The area of Kaduna basin is about four times ( $4\times$ ) the size of either Jamaare or Hadejia basin. Therefore, changes in soil, elevation and land use may have also led to inconsistencies in model performance. mHM does not incorporate a dynamic crop growth component and recognizes only three land use classes (forest, pervious and impervious). These factors

could have contributed to the mismatch in peak flow simulations. Furthermore, the poor-performing basins could be attributed to uncertainties inherent in the individual basins that constitute the multi-basin setups.

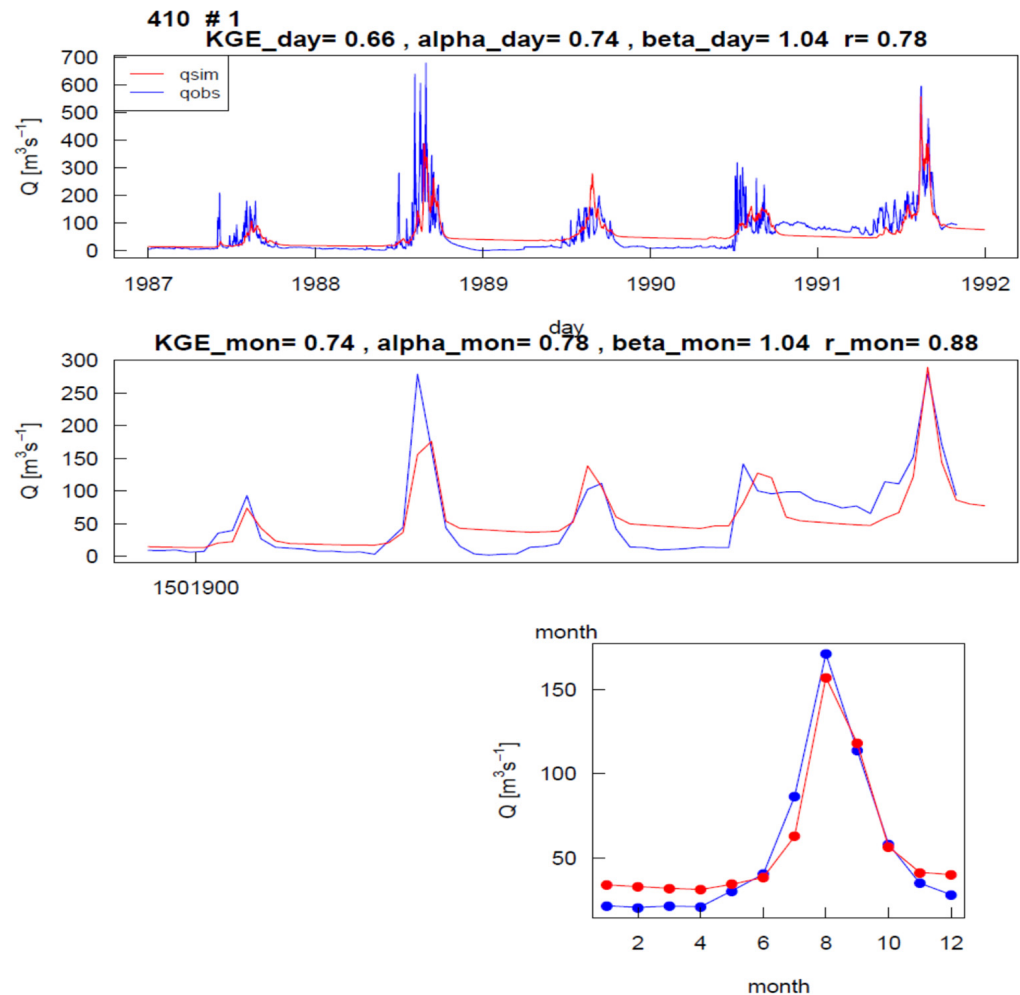


**Figure 9.** Hydrograph for Discharge Validation using mHM parameters from the independent model setup.

#### 4. Conclusions

Sparse and non-existent hydro-meteorological gauging networks have hindered hydrologic modelling in Nigeria. This has major implications for water and agricultural management at the mesoscale and at a period when hydrologic extremes (flood and drought) occasioned by climate variability occur annually in Nigeria. This study evaluates the skill of mHM for the transferability of model parameters from gauged to ungauged regions. After evaluating four grid-based precipitation products, the CHIRPS precipitation dataset was selected as model forcing to evaluate the robustness of the mHM regionalization scheme in data-sparse basins located in Northern Nigeria. Our results showed acceptable discharge simulations by using optimized parameters in contrast to default model parameters. The CHIRPS datasets produced satisfactory results during default and optimized mHM discharge simulations. For optimized mHM runs, CHIRPS and MSWEP products exhibited acceptable performance with  $KGE > 0.6$  across all basins under consideration. The sub-grid variability at the level in morphological input datasets, which characterizes the MPR technique is a major factor for satisfactory flow simulation in all basins. However, this result was not achieved when optimized parameter sets were obtained in a multi-basin configuration and transferred to an independent basin. Only the Hadejia river basin showed acceptable results when mHM was evaluated using optimized model parameter

values from another location. This inconsistency in model performance can be caused by poor representation of dam/reservoirs, lack of a plant module within the mHM structure and uncertainties inherent in model inputs.

We agree that there is a need for further mHM studies in Nigeria to exhaustively investigate the performance of model parameter transferability to ungauged basins. The paucity of discharge records limited such applicability in this aspect. It will be interesting to assess mHM hydrologic simulation performance in the same region driven by ground-measured rainfall data. This approach will reinforce the scientific understanding of the utility of the model robustness for discharge simulation in Nigeria. In addition, a multi-variable calibration scheme should be incorporated to constrain the model's internal state. This research seeks to encourage and stir interest within the Nigerian scientific community, watershed managers and government institutions/policymakers on the feasibility and applicability of the mHM-MPR scheme to support water resources management and policy-making in the light of the hydro-meteorological deficits.

**Author Contributions:** Conceptualization, K.N.O., O.R. and P.K.S.; Methodology, K.N.O., O.R., L.S. and B.T.; Software and Validation, K.N.O., O.R. and P.K.S.; Formal Analysis, K.N.O. and H.M.; Writing—original Draft, K.N.O. and O.R.; Writing—Review and Editing, K.N.O., O.R., P.K.S., B.T. and H.M.; Supervision, L.S. and B.T. All authors have read and agreed to the published version of the manuscript.

**Funding:** This research received no external funding.

**Data Availability Statement:** Most datasets used in this research were obtained from publicly accessible repositories. Interested users should check the references section for further information. Synoptic rainfall and discharge records were obtained from a government agency in Nigeria and we do not have the right to share this information.

**Acknowledgments:** The first author is a junior researcher at the Center for Development Research (ZEF), University of Bonn and acknowledges ZEF and Nnamdi Azikiwe University (NAU) for their support during his study program. This research publication was supported by the Open Access Publication Fund of the University of Bonn, Germany. We acknowledge the use of the high-performance computing (HFC) facility at the Helmholtz Centre for Environmental Research (UFZ), Leipzig, Germany for the hydrologic modelling and model input-data pre-processing aspect of this study.

**Conflicts of Interest:** The authors declare no conflict of interest.

## Appendix A

**Table A1.** List of mHM Parameters and their predictor variables.

Parameters	Description	MPR Predictor Variable
$\beta_1$	Thickness of waterfilm on the canopy surface (-)	Landcover
$\beta_2$	Threshold temperature for temperature for phase transition snow and rain ( $^{\circ}\text{C}$ )	-
$\beta_3$	Degree day factor during rainless days ( $\text{mm d}^{-1} \text{ }^{\circ}\text{C}$ )	Landcover
$\beta_4$	Rate of increase of the degree-day factor per unit of precipitation ( $\text{mm d}^{-1} \text{ }^{\circ}\text{C}$ )	-
$\beta_5$	Maximum degree-day factor reached during rainy days ( $\text{mm d}^{-1} \text{ }^{\circ}\text{C}$ )	Landcover
$\beta_6$	Maximum soil moisture content of kth root zone (mm)	Soil texture, land cover
$\beta_7$	Parameter that determines the relative contribution of rain or snowmelt to runoff (-)	Soil texture, land cover
$\beta_8$	Critical value of soil ice content above which the soil is practically impermeable	Soil texture
$\beta_9$	Shape factor of the gamma distribution (mm)	-
$\beta_{10}$	ATI threshold below which unfrozen water content reaches its minimum (K)	Soil texture

Table A1. Cont.

Parameters	Description	MPR Predictor Variable
$\beta_{11}$	ATI threshold above which no frozen water exist (K)	Soil texture
$\beta_{12}$	Minimum fraction of unfrozen water content	Soil texture
$\beta_{13}$	Weighting multiplier to estimate ATI from air temperature (-)	-
$\beta_{14}$	Maximum ponding retention in impervious areas (mm)	Land cover
$\beta_{15}$	Permanent wilting point, estimated as a fraction of max. soil moisture content (-)	Soil texture, land cover
$\beta_{16}$	Soil moisture limit above which the actual transpiration is equated with the PET (-)	Soil texture, land cover
$\beta_{17}$	Fraction of roots in the first root zone layer (-)	Land cover
$\beta_{18}$	Maximum holding capacity of the second reservoir (unsaturated zone) (mm)	Soil texture, land cover
$\beta_{19}$	Fast-recession constant (d)	Slope
$\beta_{20}$	Slow-recession constant (d)	Soil texture
$\beta_{21}$	Exponent that quantifies the degree of nonlinearity of the cell response (-)	Soil texture
$\beta_{22}$	Effective percolation rate (d)	Soil texture
$\beta_{23}$	Baseflow recession rate (d)	Geology
$\beta_{24}$	Fraction of the groundwater recharge that might be gained or lost either as deep percolation or as intercatchment groundwater flow in nonconservative catchments (-)	Geology
$\beta_{25}$	Duration of the triangular unit hydrograph (h)	Length, slope and landcover along drainage path within cell
$\beta_{26}$	Muskingum travel time parameter (h)	Length, slope and landcover of river reach
$\beta_{27}$	Muskingum attenuation parameter (-)	Slope of river reach
$\beta_{28}$	Aspect correction factor of the PET (-)	Aspect

## Appendix B

Table A2. Values of optimized global parameters for different multi-basin mHM setup.

Global Parameter	Basin 250 + basin 410	Basin 250 + Basin 572	Basin 572 + Basin 410
Canopy Interception Factor	0.2681	0.2028	0.2156
Organic Matter Content (forest)	9.8836	5.0797	6.4115
Organic Matter Content (impervious)	0.9829	0.9182	0.8356
Organic Matter Content (pervious)	4.9552	1.0180	1.0002
PTF_lower66_5_constant	0.7997	0.7729	0.7555
PTF_lower66_5_clay	0.0012	0.0012	0.0012
PTF_lower66_5_Db	-0.2504	-0.2551	-0.2642
PTF_higher66_5_constant	0.8001	0.8020	0.8934
PTF_higher66_5_clay	-0.0011	-0.0012	-0.0008
PTF_higher66_5_Db	-0.3496	-0.3493	-0.3019
PTF_Ks_constant	-0.4587	-0.5584	-0.3396
PTF_Ks_sand	0.0096	0.0199	0.0093
PTF_Ks_clay	0.0078	0.0070	0.0097
Root Fraction Coefficient (forest)	0.9021	0.9987	0.9990
Root Fraction Coefficient (impervious)	0.92534	0.9004	0.9497
Root Fraction Coefficient (pervious)	0.0881	0.0011	0.0011
Infiltration Shape Factor	1.0030	1.0048	1.0080
Impervious Storage Capacity	0.0888	0.0322	0.0746
Min Correction Factor PET	1.1272	1.2578	1.2655
Max Correction Factor PET	0.1832	0.1988	0.1960
Aspect Threshold PET	198.1908	197.6042	199.9155
Interflow Storage Capacity Factor	195.1194	194.5852	198.6782

Table A2. Cont.

Global Parameter	Basin 250 + basin 410	Basin 250 + Basin 572	Basin 572 + Basin 410
Interflow Recession (slope)	9.9847	6.7972	2.1313
Fast Interflow Recession (forest)	2.8495	2.8620	2.9520
Slow Interflow Recession (Ks)	5.2018	1.2624	5.7972
Exponent Slow Interflow	0.0532	0.0532	0.0557
Recharge Coefficient	10.5805	22.65960	9.6152
Recharge Factor (karstic)	−3.6442	−4.7927	−1.2947
Muskingum Travel Time (constant)	0.3452	0.3474	0.3487
Muskingum Travel Time (river Length)	0.0747	0.0799	0.0798
Muskingum Travel Time (river Slope)	2.0970	2.0374	2.0473
Muskingum Travel Time (impervious)	0.1008	0.0970	0.1066
Muskingum Attenuation (river Slope)	0.0101	0.0464	0.0768
GeoParam(1:)	993.6726	8.4011	974.9530
GeoParam(2:)	997.0097	987.2088	975.3943

## References

- Poméon, T.; Diekkrüger, B.; Kumar, R. Computationally Efficient Multivariate Calibration and Validation of a Grid-Based Hydrologic Model in Sparsely Gauged West African River Basins. *Water* **2018**, *10*, 1418. [[CrossRef](#)]
- Bjornlund, V.; Bjornlund, H.; Van Rooyen, A.F. Why Agricultural Production in Sub-Saharan Africa Remains Low Compared to the Rest of the World—A Historical Perspective. *Int. J. Water Resour. Dev.* **2020**, *36*, S20–S53. [[CrossRef](#)]
- Dembélé, M.; Zwart, S.J. Evaluation and Comparison of Satellite-Based Rainfall Products in Burkina Faso, West Africa. *Int. J. Remote Sens.* **2016**, *37*, 3995–4014. [[CrossRef](#)]
- Chapman, S.; E Birch, C.; Pope, E.; Sallu, S.; Bradshaw, C.; Davie, J.; Marsham, J.H. Impact of Climate Change on Crop Suitability in Sub-Saharan Africa in Parameterized and Convection-Permitting Regional Climate Models. *Environ. Res. Lett.* **2020**, *15*, 094086. [[CrossRef](#)]
- Emediegwu, L.E.; Wossink, A.; Hall, A. The Impacts of Climate Change on Agriculture in Sub-Saharan Africa: A Spatial Panel Data Approach. *World Dev.* **2022**, *158*, 105967. [[CrossRef](#)]
- Ofori, S.A.; Cobbina, S.J.; Obiri, S. Climate Change, Land, Water, and Food Security: Perspectives From Sub-Saharan Africa. *Front. Sustain. Food Syst.* **2021**, *5*, 218. [[CrossRef](#)]
- Caldera, H.P.G.M.; Piyathisse, V.R.P.C.; Nandalal, K.D.W. A Comparison of Methods of Estimating Missing Daily Rainfall Data. *Eng. J. Inst. Eng. Sri Lanka* **2016**, *49*, 1–8. [[CrossRef](#)]
- Akinsanola, A.A.; Ajayi, V.O.; Adejare, A.T.; Adeyeri, O.E.; Gbode, I.E.; Ogunjobi, K.O.; Nikulin, G.; Abolude, A.T. Evaluation of Rainfall Simulations over West Africa in Dynamically Downscaled CMIP5 Global Circulation Models. *Theor. Appl. Climatol.* **2018**, *132*, 437–450. [[CrossRef](#)]
- Ogbu, K.N.; Houngue, N.R.; Gbode, I.E.; Tischbein, B. Performance Evaluation of Satellite-Based Rainfall Products over Nigeria. *Climate* **2020**, *8*, 103. [[CrossRef](#)]
- Houngue, N.R.; Ogbu, K.N.; Almoradie, A.D.S.; Evers, M. Evaluation of the Performance of Remotely Sensed Rainfall Datasets for Flood Simulation in the Transboundary Mono River Catchment, Togo and Benin. *J. Hydrol. Reg. Stud.* **2021**, *36*, 100875. [[CrossRef](#)]
- Anyadike, R.N.C. Seasonal and Annual Rainfall Variations over Nigeria. *Int. J. Climatol.* **1993**, *13*, 567–580. [[CrossRef](#)]
- Animashaun, I.M.; Oguntunde, P.G.; Akinwumiju, A.S.; Olubanjo, O.O. Rainfall Analysis over the Niger Central Hydrological Area, Nigeria: Variability, Trend, and Change Point Detection. *Sci. Afr.* **2020**, *8*, e00419. [[CrossRef](#)]
- Okafor, G.C.; Ogbu, K.N. Assessment of the Impact of Climate Change on the Freshwater Availability of Kaduna River Basin, Nigeria. *J. Water Land Dev.* **2018**, *38*, 105–114. [[CrossRef](#)]
- Usman, M.; Nichol, J.E.; Ibrahim, A.T.; Buba, L.F. A Spatio-Temporal Analysis of Trends in Rainfall from Long Term Satellite Rainfall Products in the Sudano Sahelian Zone of Nigeria. *Agric. For. Meteorol.* **2018**, *260–261*, 273–286. [[CrossRef](#)]
- Akande, A.; Costa, A.C.; Mateu, J.; Henriques, R. Geospatial Analysis of Extreme Weather Events in Nigeria (1985–2015) Using Self-Organizing Maps. *Adv. Meteorol.* **2017**, *2017*, 8576150. [[CrossRef](#)]
- Adeyeri, O.E.; Lawin, A.E.; Laux, P.; Ishola, K.A.; Ige, S.O. Analysis of Climate Extreme Indices over the Komadugu-Yobe Basin, Lake Chad Region: Past and Future Occurrences. *Weather. Clim. Extrem.* **2019**, *23*. [[CrossRef](#)]
- Ngene, B.U.; Nwafor, C.O.; Bamigboye, G.O.; Ogiyiye, A.S.; Ogundare, J.O.; Akpan, V.E. Assessment of Water Resources Development and Exploitation in Nigeria: A Review of Integrated Water Resources Management Approach. *Heliyon* **2021**, *7*, 1–10. [[CrossRef](#)]
- Ezenwaji, E.E.; Eduputa, B.M.; Ogbuozobe, J.E. Employing Water Demand Management Option for the Improvement of Water Supply and Sanitation in Nigeria. *J. Water Resour. Prot.* **2015**, *7*, 624–635. [[CrossRef](#)]
- Shiru, M.S.; Shahid, S.; Park, I. Projection of Water Availability and Sustainability in Nigeria Due to Climate Change. *Sustainability* **2021**, *13*, 6284. [[CrossRef](#)]

20. Dembélé, M.; Schaeffli, B.; Van De Giesen, N.; Mariéthoz, G. Suitability of 17 Gridded Rainfall and Temperature Datasets for Large-Scale Hydrological Modelling in West Africa. *Hydrol. Earth Syst. Sci.* **2020**, *24*, 5379–5406. [[CrossRef](#)]
21. Camici, S.; Massari, C.; Ciabatta, L.; Marchesini, I.; Brocca, L. Which Rainfall Score Is More Informative about the Performance in River Discharge Simulation? A Comprehensive Assessment on 1318 Basins over Europe. *Hydrol. Earth Syst. Sci.* **2020**, *24*, 4869–4885. [[CrossRef](#)]
22. Trinh-Tuan, L.; Matsumoto, J.; Ngo-Duc, T.; Nodzu, M.I.; Inoue, T. Evaluation of Satellite Precipitation Products over Central Vietnam. *Prog. Earth Planet. Sci.* **2019**, *6*, 54. [[CrossRef](#)]
23. Mbaye, M.L.; Haensler, A.; Hagemann, S.; Gaye, A.T.; Moseley, C.; Afouda, A. Impact of Statistical Bias Correction on the Projected Climate Change Signals of the Regional Climate Model REMO over the Senegal River Basin. *Int. J. Climatol.* **2016**, *36*, 2035–2049. [[CrossRef](#)]
24. Camberlin, P.; Barraud, G.; Bigot, S.; Dewitte, O.; Makanzu Imwangana, F.; Maki Mateso, J.; Martiny, N.; Monsieurs, E.; Moron, V.; Pellarin, T.; et al. Evaluation of Remotely Sensed Rainfall Products over Central Africa. *Q. J. R. Meteorol. Soc.* **2019**, *145*, 2115–2138. [[CrossRef](#)]
25. Raimonet, M.; Oudin, L.; Thieu, V.; Silvestre, M.; Vautard, R.; Rabouille, C.; Le Moigne, P. Evaluation of Gridded Meteorological Datasets for Hydrological Modeling. *J. Hydrometeorol.* **2017**, *18*, 3027–3041. [[CrossRef](#)]
26. Hassan, I.; Kalin, R.M.; White, C.J.; Aladejana, J.A. Evaluation of Daily Gridded Meteorological Datasets over the Niger Delta Region of Nigeria and Implication to Water Resources Management. *Atmos. Clim. Sci.* **2020**, *10*, 21–39. [[CrossRef](#)]
27. Contractor, S.; Alexander, L.V.; Donat, M.G.; Herold, N. How Well Do Gridded Datasets of Observed Daily Precipitation Compare over Australia? *Adv. Meteorol.* **2015**, *2015*, 325718. [[CrossRef](#)]
28. Nhi, P.T.T.; Khoi, D.N.; Hoan, N.X. Evaluation of Five Gridded Rainfall Datasets in Simulating Streamflow in the Upper Dong Nai River Basin, Vietnam. *Int. J. Digit. Earth* **2019**, *12*, 311–327. [[CrossRef](#)]
29. Sun, Q.; Miao, C.; Duan, Q.; Ashouri, H.; Sorooshian, S.; Hsu, K. A Review of Global Precipitation Data Sets: Data Sources, Estimation, and Intercomparisons. *Rev. Geophys.* **2018**, *56*, 79–107. [[CrossRef](#)]
30. Dinku, T.; Funk, C.; Peterson, P.; Maidment, R.; Tadesse, T.; Gadain, H.; Ceccato, P. Validation of the CHIRPS Satellite Rainfall Estimates over Eastern Africa. *Q. J. R. Meteorol. Soc.* **2018**, *144*, 292–312. [[CrossRef](#)]
31. Hersbach, H.; Bell, B.; Berrisford, P.; Hirahara, S.; Horányi, A.; Muñoz-Sabater, J.; Nicolas, J.; Peubey, C.; Radu, R.; Schepers, D.; et al. The ERA5 Global Reanalysis. *Q. J. R. Meteorol. Soc.* **2020**, *146*, 1999–2049. [[CrossRef](#)]
32. Bitew, M.M.; Gebremichael, M. Evaluation of Satellite Rainfall Products through Hydrologic Simulation in a Fully Distributed Hydrologic Model. *Water Resour. Res.* **2011**, *47*, 1–11. [[CrossRef](#)]
33. Samaniego, L.; Kumar, R.; Jackisch, C. Predictions in a Data-Sparse Region Using a Regionalized Grid-Based Hydrologic Model Driven by Remotely Sensed Data. *Hydrol. Res.* **2011**, *42*, 338–355. [[CrossRef](#)]
34. Schuol, J.; Abbaspour, K.C.; Srinivasan, R.; Yang, H. Estimation of Freshwater Availability in the West African Sub-Continent Using the SWAT Hydrologic Model. *J. Hydrol.* **2008**, *352*, 30–49. [[CrossRef](#)]
35. Poméon, T.; Diekkrüger, B.; Springer, A.; Kusche, J.; Eicker, A. Multi-Objective Validation of SWAT for Sparsely-Gauged West African River Basins - A Remote Sensing Approach. *Water* **2018**, *10*, 451. [[CrossRef](#)]
36. Xie, H.; Longuevergne, L.; Ringler, C.; Scanlon, B.R. Calibration and Evaluation of a Semi-Distributed Watershed Model of Sub-Saharan Africa Using GRACE Data. *Hydrol. Earth Syst. Sci.* **2012**, *16*, 3083–3099. [[CrossRef](#)]
37. Fujihara, Y.; Yamamoto, Y.; Tsujimoto, Y.; Sakagami, J.-I. Discharge Simulation in a Data-Scarce Basin Using Reanalysis and Global Precipitation Data: A Case Study of the White Volta Basin. *J. Water Resour. Prot.* **2014**, *06*, 1316–1325. [[CrossRef](#)]
38. Poméon, T.; Jackisch, D.; Diekkrüger, B. Evaluating the Performance of Remotely Sensed and Reanalysed Precipitation Data over West Africa Using HBV Light. *J. Hydrol.* **2017**, *547*, 222–235. [[CrossRef](#)]
39. Samaniego, L.; Kumar, R.; Attinger, S. Multiscale Parameter Regionalization of a Grid-Based Hydrologic Model at the Mesoscale. *Water Resour. Res.* **2010**, *46*, 1–25. [[CrossRef](#)]
40. Tegegne, G.; Park, D.K.; Kim, Y.O. Comparison of Hydrological Models for the Assessment of Water Resources in a Data-Scarce Region, the Upper Blue Nile River Basin. *J. Hydrol. Reg. Stud.* **2017**, *14*, 49–66. [[CrossRef](#)]
41. Beven, K. How Far Can We Go in Distributed Hydrological Modelling? *Hydrol. Earth Syst. Sci.* **2001**, *5*, 1–12. [[CrossRef](#)]
42. Beven, K. Towards a Coherent Philosophy for Modelling the Environment. *Proc. R. Soc. Lond. Ser. A Math. Phys. Eng. Sci.* **2002**, *454*, 2465–2484. [[CrossRef](#)]
43. Schoups, G.; Van De Giesen, N.C.; Savenije, H.H.G. Model Complexity Control for Hydrologic Prediction. *Water Resour. Res.* **2008**, *44*, 1–14. [[CrossRef](#)]
44. Kumar, R.; Samaniego, L.; Attinger, S. Implications of Distributed Hydrologic Model Parameterization on Water Fluxes at Multiple Scales and Locations. *Water Resour. Res.* **2013**, *49*, 360–379. [[CrossRef](#)]
45. Ocio, D.; Beskeen, T.; Smart, K. Fully Distributed Hydrological Modelling for Catchmentwide Hydrological Data Verification. *Hydrol. Res.* **2019**, *50*, 1520–1534. [[CrossRef](#)]
46. Hrachowitz, M.; Savenije, H.H.G.; Blöschl, G.; McDonnell, J.J.; Sivapalan, M.; Pomeroy, J.W.; Arheimer, B.; Blume, T.; Clark, M.P.; Ehret, U.; et al. A Decade of Predictions in Ungauged Basins (PUB)—A Review. *Hydrol. Sci. J.* **2013**, *58*, 1198–1255. [[CrossRef](#)]
47. Golian, S.; Murphy, C.; Meresa, H. Regionalization of Hydrological Models for Flow Estimation in Ungauged Catchments in Ireland. *J. Hydrol. Reg. Stud.* **2021**, *36*, 100859. [[CrossRef](#)]

48. Arnold, J.G.; Srinivasan, R.; Muttiah, R.S.; Williams, J.R. LARGE AREA HYDROLOGIC MODELING AND ASSESSMENT PART I: MODEL DEVELOPMENT. *J. Am. Water Resour. Assoc.* **1998**, *34*, 73–89. [[CrossRef](#)]
49. Ndulue, E.L.; Ezenne, G.I.; Mbajjorgu, C.C.; Ogwo, V.; Ogbu, K.N. Hydrological Modelling of Upper Ebonyi Watershed Using the SWAT Model. *Int. J. Hydrol. Sci. Technol.* **2018**, *8*, 120–133. [[CrossRef](#)]
50. Odusanya, A.E.; Mehdi, B.; Schürz, C.; Oke, A.O.; Awokola, O.S.; Awomeso, J.A.; Adejuwon, J.O.; Schulz, K. Multi-Site Calibration and Validation of SWAT with Satellite-Based Evapotranspiration in a Data-Sparse Catchment in Southwestern Nigeria. *Hydrol. Earth Syst. Sci.* **2019**, *23*, 1113–1144. [[CrossRef](#)]
51. Rathjens, H.; Bieger, K.; Srinivasan, R.; Arnold, J.G. CMhyd User Manual Documentation for Preparing Simulated Climate Change Data for Hydrologic Impact Studies. 2016, p. 16. Available online: [https://swat.tamu.edu/media/115265/bias\\_cor\\_man.pdf](https://swat.tamu.edu/media/115265/bias_cor_man.pdf) (accessed on 25 August 2020).
52. Guug, S.S.; Abdul-Ganiyu, S.; Kasei, R.A. Application of SWAT Hydrological Model for Assessing Water Availability at the Sherigu Catchment of Ghana and Southern Burkina Faso. *HydroResearch* **2020**, *3*, 124–133. [[CrossRef](#)]
53. Zettam, A.; Taleb, A.; Sauvage, S.; Boithias, L.; Belaidi, N.; Sanchez-Perez, J.M. Applications of a SWAT Model to Evaluate the Contribution of the Tafna Catchment (North-West Africa) to the Nitrate Load Entering the Mediterranean Sea. *Environ. Monit. Assess.* **2020**, *192*, 510. [[CrossRef](#)]
54. Bizuneh, B.B.; Moges, M.A.; Sinshaw, B.G.; Kerebih, M.S. SWAT and HBV Models' Response to Streamflow Estimation in the Upper Blue Nile Basin, Ethiopia. *Water-Energy Nexus* **2021**, *4*, 41–53. [[CrossRef](#)]
55. Hundecha, Y.; Bárdossy, A. Modeling of the Effect of Land Use Changes on the Runoff Generation of a River Basin through Parameter Regionalization of a Watershed Model. *J. Hydrol.* **2004**, *292*, 281–295. [[CrossRef](#)]
56. Rakovec, O.; Kumar, R.; Attinger, S.; Samaniego, L. Improving the Realism of Hydrologic Model Functioning through Multivariate Parameter Estimation. *Water Resour. Res.* **2016**, *52*, 7779–7792. [[CrossRef](#)]
57. Zink, M.; Kumar, R.; Cuntz, M.; Samaniego, L. A High-Resolution Dataset of Water Fluxes and States for Germany Accounting for Parametric Uncertainty. *Hydrol. Earth Syst. Sci.* **2017**, *21*, 1769–1790. [[CrossRef](#)]
58. Samaniego, L.; Thober, S.; Wanders, N.; Pan, M.; Rakovec, O.; Sheffield, J.; Wood, E.F.; Prudhomme, C.; Rees, G.; Houghton-Carr, H.; et al. Hydrological Forecasts and Projections for Improved Decision-Making in the Water Sector in Europe. *Bull. Am. Meteorol. Soc.* **2019**, *100*, 2451–2471. [[CrossRef](#)]
59. Rakovec, O.; Mizukami, N.; Kumar, R.; Newman, A.J.; Thober, S.; Wood, A.W.; Clark, M.P.; Samaniego, L. Diagnostic Evaluation of Large-Domain Hydrologic Models Calibrated Across the Contiguous United States. *J. Geophys. Res. Atmos.* **2019**, *124*, 13991–14007. [[CrossRef](#)]
60. Saha, T.R.; Shrestha, P.K.; Rakovec, O.; Thober, S.; Samaniego, L. A Drought Monitoring Tool for South Asia. *Environ. Res. Lett.* **2021**, *16*, 054014. [[CrossRef](#)]
61. Dembélé, M.; Hrachowitz, M.; Savenije, H.H.G.; Mariéthoz, G.; Schaeffli, B. Improving the Predictive Skill of a Distributed Hydrological Model by Calibration on Spatial Patterns With Multiple Satellite Data Sets. *Water Resour. Res.* **2020**, *56*. [[CrossRef](#)]
62. Dembélé, M.; Vrac, M.; Ceperley, N.; Zwart, S.; Larsen, J.; Dadson, S.; Mariéthoz, G.; Schaeffli, B. Contrasting Dynamics of Hydrological Processes in the Volta River Basin under Global Warming. *Hydrol. Earth Syst. Sci. Discuss.* **2022**, *26*, 1481–1506. [[CrossRef](#)]
63. Omotosho, J.B.; Abiodun, B.J. A Numerical Study of Moisture Build-up and Rainfall over West Africa. *Meteorol. Appl.* **2007**, *14*, 209–225. [[CrossRef](#)]
64. Gbode, I.E.; Adeyeri, O.E.; Menang, K.P.; Intsiful, J.D.K.; Ajayi, V.O.; Omotosho, J.A.; Akinsanola, A.A. Observed Changes in Climate Extremes in Nigeria. *Meteorol. Appl.* **2019**, *26*, 642–654. [[CrossRef](#)]
65. Odunuga, S.; Okeke, I.; Omojola, A.; Oyebande, L. Hydro-Climatic Variability of the Hadejia-Jama'are River Systems in North-Central Nigeria. *IAHS-AISH Publication* **2011**, *344*, 163–168.
66. U.S Geological Survey USGS EROS Archive—Digital Elevation—Global Multi-Resolution Terrain Elevation Data 2010 (GMTED2010) | U.S. Geological Survey. Available online: <https://www.usgs.gov/centers/eros/science/usgs-eros-archive-digital-elevation-global-multi-resolution-terrain-elevation> (accessed on 25 August 2020).
67. Lindström, G.; Johansson, B.; Persson, M.; Gardelin, M.; Bergström, S. Development and Test of the Distributed HBV-96 Hydrological Model. *J. Hydrol.* **1997**, *201*, 272–288. [[CrossRef](#)]
68. Liang, X.; Lettenmaier, D.P.; Wood, E.F.; Burges, S.J. A Simple Hydrologically Based Model of Land Surface Water and Energy Fluxes for General Circulation Models. *J. Geophys. Res. Atmos.* **1994**, *99*, 14415–14428. [[CrossRef](#)]
69. Kumar, R.; Samaniego, L.; Attinger, S. The Effects of Spatial Discretization and Model Parameterization on the Prediction of Extreme Runoff Characteristics. *J. Hydrol.* **2010**, *392*, 54–69. [[CrossRef](#)]
70. Scheppe, R.; Thober, S.; Müller, S.; Kelbling, M.; Kumar, R.; Attinger, S.; Samaniego, L. MPR 1.0: A Stand-Alone Multiscale Parameter Regionalization Tool for Improved Parameter Estimation of Land Surface Models. *Geosci. Model. Dev.* **2022**, *15*, 859–882. [[CrossRef](#)]
71. Samaniego, L.; Kumar, R.; Thober, S.; Rakovec, O.; Zink, M.; Wanders, N.; Eisner, S.; Müller Schmied, H.; Sutanudjaja, E.; Warrach-Sagi, K.; et al. Toward Seamless Hydrologic Predictions across Spatial Scales. *Hydrol. Earth Syst. Sci.* **2017**, *21*, 4323–4346. [[CrossRef](#)]
72. Mizukami, N.; Clark, M.P.; Newman, A.J.; Wood, A.W.; Gutmann, E.D.; Nijssen, B.; Rakovec, O.; Samaniego, L. Towards Seamless Large-Domain Parameter Estimation for Hydrologic Models. *Water Resour. Res.* **2017**, *53*, 8020–8040. [[CrossRef](#)]

73. Imhoff, R.O.; van Verseveld, W.J.; van Osnabrugge, B.; Weerts, A.H. Scaling Point-Scale (Pedo)Transfer Functions to Seamless Large-Domain Parameter Estimates for High-Resolution Distributed Hydrologic Modeling: An Example for the Rhine River. *Water Resour. Res.* **2020**, *56*, e2019WR026807. [[CrossRef](#)]
74. Hartmann, J.; Moosdorf, N. The New Global Lithological Map Database GLiM: A Representation of Rock Properties at the Earth Surface. *Geochem. Geophys. Geosystems* **2012**, *13*, 1–37. [[CrossRef](#)]
75. Hengl, T.; Mendes de Jesus, J.; Heuvelink, G.B.M.; Ruiperez Gonzalez, M.; Kilibarda, M.; Blagotić, A.; Shangquan, W.; Wright, M.N.; Geng, X.; Bauer-Marschallinger, B.; et al. SoilGrids250m: Global Gridded Soil Information Based on Machine Learning. *PLOS ONE* **2017**, *12*, e0169748. [[CrossRef](#)]
76. Bontemps, S.; Herold, M.; Kooistra, L.; Van Groenestijn, A.; Hartley, A.; Arino, O.; Moreau, I.; Defourny, P. Global Land Cover Dataset for Climate Models Revisiting Land Cover Observations to Address the Needs of the Climate Modelling Community Global Land Cover Dataset for Climate Models. *Biogeosciences Discuss* **2011**, *8*, 7713–7740. [[CrossRef](#)]
77. Zhu, Z.; Bi, J.; Pan, Y.; Ganguly, S.; Anav, A.; Xu, L.; Samanta, A.; Piao, S.; Nemani, R.R.; Myneni, R.B. Global Data Sets of Vegetation Leaf Area Index (LAI)3g and Fraction of Photosynthetically Active Radiation (FPAR)3g Derived from Global Inventory Modeling and Mapping Studies (GIMMS) Normalized Difference Vegetation Index (NDVI3G) for the Period 1981 to 2011. *Remote Sens.* **2013**, *5*, 927–948. [[CrossRef](#)]
78. Funk, C.; Peterson, P.; Landsfeld, M.; Pedreros, D.; Verdin, J.; Shukla, S.; Husak, G.; Rowland, J.; Harrison, L.; Hoell, A.; et al. The Climate Hazards Infrared Precipitation with Stations —A New Environmental Record for Monitoring Extremes. *Sci. Data.* **2015**, *2*. [[CrossRef](#)]
79. Schamm, K.; Ziese, M.; Becker, A.; Finger, P.; Meyer-Christoffer, A.; Schneider, U.; Schröder, M.; Stender, P. Global Gridded Precipitation over Land: A Description of the New GPCC First Guess Daily Product. *Earth Syst. Sci. Data* **2014**, *6*, 49–60. [[CrossRef](#)]
80. Beck, H.E.; Wood, E.F.; Pan, M.; Fisher, C.K.; Miralles, D.G.; Van Dijk, A.I.J.M.; McVicar, T.R.; Adler, R.F. MSWEP V2 Global 3-Hourly 0.1° Precipitation: Methodology and Quantitative Assessment. *Bull. Am. Meteorol. Soc.* **2019**, *100*, 473–500. [[CrossRef](#)]
81. Gupta, H.V.; Kling, H.; Yilmaz, K.K.; Martinez, G.F. Decomposition of the Mean Squared Error and NSE Performance Criteria: Implications for Improving Hydrological Modelling. *J. Hydrol.* **2009**, *377*, 80–91. [[CrossRef](#)]
82. Moriasi, D.N.; Gitau, M.W.; Pai, N.; Daggupati, P.; Gitau, M.W.; Member, A.; Moriasi, D.N. Hydrologic and water quality models: Performance measures and evaluation criteria. *Trans. ASABE* **2015**, *58*, 1763–1785. [[CrossRef](#)]
83. Hargreaves, G.H.; Samani, Z.A. Reference Crop Evapotranspiration from Temperature. *Appl. Eng. Agric.* **1985**, *1*, 96–99. [[CrossRef](#)]
84. Knoben, W.J.M.; Freer, J.E.; Woods, R.A. Technical Note: Inherent Benchmark or Not? Comparing Nash-Sutcliffe and Kling-Gupta Efficiency Scores. *Hydrol. Earth Syst. Sci.* **2019**, *23*, 4323–4331. [[CrossRef](#)]
85. Duan, Q.Y.; Gupta, V.K.; Sorooshian, S. Shuffled Complex Evolution Approach for Effective and Efficient Global Minimization. *J. Optim. Theory Appl.* **1993**, *76*, 501–521. [[CrossRef](#)]
86. Ingber, L. Simulated Annealing: Practice versus Theory. *Math. Comput. Model.* **1993**, *18*, 29–57. [[CrossRef](#)]
87. Eberhart, R.; Kennedy, J. New Optimizer Using Particle Swarm Theory. In Proceedings of the Sixth International Symposium on Micro Machine and Human Science, Nagoya, Japan, 4–6 October 1995; pp. 39–43.
88. Hansen, N. The CMA Evolution Strategy: A Comparing Review. In *Towards a New Evolutionary Computation*; Springer: Berlin/Heidelberg, Germany, 2007; pp. 75–102.
89. Tolson, B.A.; Shoemaker, C.A. Dynamically Dimensioned Search Algorithm for Computationally Efficient Watershed Model Calibration. *Water Resour. Res.* **2007**, *43*, 1–16. [[CrossRef](#)]
90. Salaudeen, A.; Ismail, A.; Adeogun, B.K.; Ajibike, M.A.; Zubairu, I. Evaluation of Ground-Based, Daily, Gridded Precipitation Products for Upper Benue River Basin, Nigeria. *Eng. Appl. Sci. Res.* **2021**, *48*, 397–405. [[CrossRef](#)]
91. Ogunjo, S.T.; Olusegun, C.F.; Fuwape, I.A. Evaluation of Monthly Precipitation Data from Three Gridded Climate Data Products over Nigeria. *Remote Sens. Earth Syst. Sci.* **2022**, *5*, 119–128. [[CrossRef](#)]
92. Zandler, H.; Haag, I.; Samimi, C. Evaluation Needs and Temporal Performance Differences of Gridded Precipitation Products in Peripheral Mountain Regions. *Sci. Rep.* **2019**, *9*, 15118. [[CrossRef](#)]
93. Akinyemi, D.F.; Ayanlade, O.S.; Nwaezeigwe, J.O.; Ayanlade, A. A Comparison of the Accuracy of Multi-Satellite Precipitation Estimation and Ground Meteorological Records Over Southwestern Nigeria. *Remote Sens. Earth Syst. Sci.* **2020**, *3*, 1–12. [[CrossRef](#)]
94. Satgé, F.; Ruelland, D.; Bonnet, M.-P.; Molina, J.; Pillco, R. Consistency of Satellite-Based Precipitation Products in Space and over Time Compared with Gauge Observations and Snow- Hydrological Modelling in the Lake Titicaca Region. *Hydrol. Earth Syst. Sci.* **2019**, *23*, 595–619. [[CrossRef](#)]
95. Satgé, F.; Defrance, D.; Sultan, B.; Bonnet, M.P.; Seyler, F.; Rouché, N.; Pierron, F.; Paturel, J.E. Evaluation of 23 Gridded Precipitation Datasets across West Africa. *J. Hydrol.* **2020**, *581*, 124412. [[CrossRef](#)]
96. Beck, H.E.; Vergopolan, N.; Pan, M.; Levizzani, V.; Van Dijk, A.I.J.M.; Weedon, G.P.; Brocca, L.; Pappenberger, F.; Huffman, G.J.; Wood, E.F. Global-Scale Evaluation of 22 Precipitation Datasets Using Gauge Observations and Hydrological Modeling. *Hydrol. Earth Syst. Sci.* **2017**, *21*, 6201–6217. [[CrossRef](#)]
97. Zelelew, M.B.; Alfredsen, K. Transferability of Hydrological Model Parameter Spaces in the Estimation of Runoff in Ungauged Catchments. *Hydrol. Sci. J.* **2014**, *59*, 1470–1490. [[CrossRef](#)]